THE UNIVERSITY of TENNESSEE at CHATTANOOGA
COLLEGE of ENGINEERING and COMPUTER SCIENCE

SIMCENTER
NATIONAL CENTER for COMPUTATIONAL ENGINEERING

A Review of Computational Ship Hydrodynamics

A Technical Report by

Robert V. Wilson

UTC-CECS-SimCenter-2008-03
September 2008

GRADUATE SCHOOL OF COMPUTATIONAL ENGINEERING
701 East M.L. King Boulevard • Chattanooga, TN 37403

The University of Tennessee at Chattanooga
College of Engineering and Computer Science

SimCenter: National Center for Computational Engineering

A REVIEW OF COMPUTATIONAL SHIP HYDRODYNAMICS

A Technical Report by

Robert V. Wilson

Submitted to:

Department of Mechanical Engineering
Old Dominion University
238 Kaufman Hall
Norfolk, VA 23529-0247

TABLE OF CONTENTS

1 State-of-the-Art for Computational Ship Hydrodynamics

1.1 Early Workshops

A series of international workshops on computational ship hydrodynamics (CSH) has been held dating back to 1980, to access the current state-of-the-art in the field and to identify short comings and future research directions for solution methodologies. Typical procedures call for participants to perform computational fluid dynamics (CFD) solutions for standardized ship test cases and to submit comparison figures of CFD results and experimental data prior to the workshop. Most of the experimental data for the test cases are available to participants prior to the workshops, although data for a few cases have been withheld until after the submission of the computational results. During the meeting, papers are presented and discussions are held to access the accuracy, strengths, and weaknesses of the various solutions and methodologies.

The focus of the first workshop (1980 SSPA-ITTC Ship Boundary Layer Workshop) was on ship boundary layers with computations based on solution of the simplified boundary layer equations. Computations for two model ship test cases were submitted from 17 groups. The general conclusion was that most methods were able to predict the boundary layer over most of the hull for engineering accuracy, but that all methods failed completely in predicting flow at the stern and into the wake. A decade later, computations at the second workshop (1990 SSPA-CTH-IIHR Workshop on Ship Viscous Flow) were based mainly on the Reynolds averaged Navier-Stokes (RANS) equations and focused on ship stern and wake flows. Computations for the HSVA and "Mystery" tankers were submitted by 19 groups. Unlike the first workshop, most methods were able to capture the gross features of the flow near the propeller plane. However, results inside the propeller disk were less satisfactory due to inaccurate prediction of the bilge vortex and the resultant characteristic "hook" shape in the boundary layer.

Unlike the first two workshops where a double model assumption was used, CFD Workshop Tokyo 1994 added viscous flow prediction about the Series 60 cargo ship with free-surface to the two test cases from the previous workshop. Among the eight papers, many RANS simulations accurately predicted the Series 60 wave profile, but all showed

moderate to major damping of the wave pattern away from the hull due to insufficient grid resolution of the diverging and transverse wave systems and excessive numerical dissipation.

1.2 Gothenburg 2000: A Workshop on Numerical Ship Hydrodynamics

In the six years between the first three workshops and the fourth, Gothenburg 2000 Workshop on Numerical Ship Hydrodynamics (G2K), rapid development of solution methodologies took place, with CSH applications extended to include complex geometry (e.g., sonar dome, transom stern, appendages, advanced propulsors), complex physics (e.g., non-linear turbulence modeling, breaking waves, two-phase flow, thermal effects), and complex environment (e.g., wind, incident waves, ship motions, maneuvers). Gothenburg 2000 workshop details such as numerical and physical modeling methodology, code nomenclature, and computational grids are given in Larsson et al. (2002) and Larsson et al. (2003). The reader is referred to these works when details are omitted in the following discussion.

Older designs used in the previous three workshops were replaced with modern ship test cases: the KRISO Tanker Ship (KVLCC2), the KRISO Container Ship (KCS), and the U.S. Navy Combatant (DTMB 5415), as shown in Figure 1. The KRISO tanker ship represents a full hull form which generates strong stern vortices due to flow contraction at the aft end of the ship. The validation data for this case are stern flow mean velocity and turbulence at zero Froude number (i.e., wind tunnel measurements), surface pressure, and limiting streamlines. The focus of the KCS case is on prediction of propeller-hull interaction and free surface with validation data consisting of stern flow mean velocities and surface pressure with and without an operating propeller, resistance without propeller, and prediction of the self-propulsion point. Finally, predictive capability of RANS solvers for free surface flow around a transom stern hull is tested with the bare hull DTMB 5415. Detailed validation data includes stern flow velocities, wave elevation and profile along the hull, and ship resistance. A detailed description of the test case conditions can be found at the workshop website: http://www.iihr.uiowa.edu/gothenburg2000/. Workshop organizers also required participants to access numerical and modeling uncertainties in their solutions.

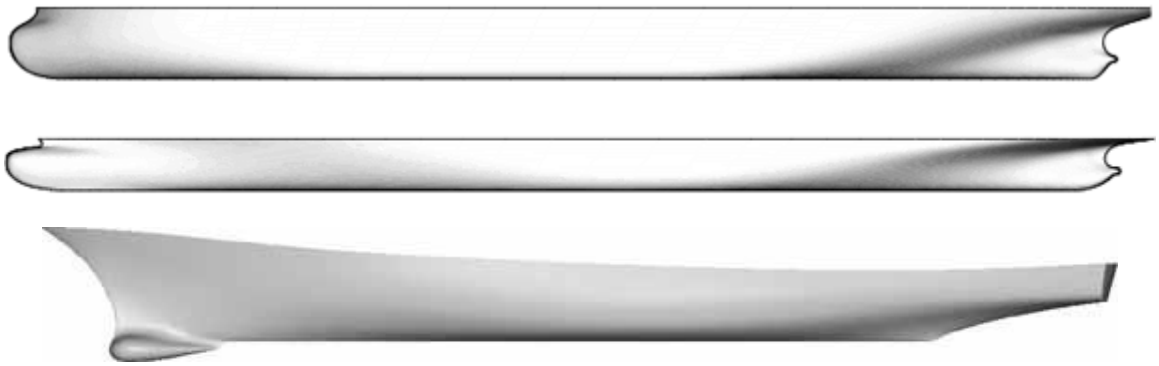

Figure 1 Test case geometries for Gothenburg 2000 Workshop: KVLCC2 tanker (top), KCS container (middle), and DTMB 5415 surface combatant (bottom).

With regard to computational software, codes developed by larger institutes and commercial companies largely replaced PhD thesis codes. Of the 20 groups that participated in the fourth workshop, 16 different RANS codes were utilized and developed by five academic institutes, eight industrial institutes, and three commercial companies, as summarized in Table 1. In contrast with previous workshops, many codes had a free surface prediction capability and utilized two-equation turbulence models with fewer tunable constants, while two groups presented results using Reynolds stress turbulence models.

Table 1 Gothenburg 2000 workshop codes, organizations, and submissions.

						Test case		
Code number	Code	Organization number	Organization	Country	Acronym	KVLCC2	KCS	5415
1	FLUENT	1	Chalmers University of Technology	Sweden	CTU	Y		
		2	Fluent	USA	FLUENT	Y		
2	HORUS	3	Ecole Centrale de Nantes	France	ECN	Y		
3	PARNASSOS	4	Maritime Research Institute Netherlands/Instituto Superior Técnico (Netherlands/Portugal)	Netherlands	MARIN/IST	Y	w/o	
4	CFX	5	Southampton University	UK	SOTON	Y		
		6	Potsdam Ship Model Basin/AEA Technology	Germany	SVA/AEA	Y	w/	
		7	Defence Research Agency	UK	DERA			Y
5	SURF	8	Ship Research Institute	Japan	SRI	Y	w/o	
6	NEPTUNE	9	Ship Research Institute	Japan	SRI	Y		
7	UVW	10	United Ship Design and Development Center	Taiwan	USDDC	Y	w/o, w/	
8	WAVIS	11	Korean Institute of Ships and Ocean Engineering	Korea	KRISO	Y		
9	NEPTUN	12	Hamburg Ship Model Tank	Germany	HSVA		w/o	
10	COMET	13	Hamburg Ship Model Tank	Germany	HSVA		w/o	
		14	National Taiwan University	Taiwan	NTU			Y
11	FINFLO	15	Helsinki University of Technology–Technical Research Center of Finland	Finland	HUT-VTT		w/o	Y
12	FLOWPACK	16	Osaka Prefecture University	Japan	OPU		w/o, w/	
13	ICARE	17	Ecole Centrale de Nantes	France	ECN			Y
14	CFDSHIP	18	Iowa Institute of Hydraulic Research	USA	IIHR			Y
15	MGSHIP	19	Istituto Nazionale per Studi ed Esperienze di Architettura Navale	Italy	INSEAN			Y
16	UNCLE	20	Mississippi State University	USA	MSU	Y		Y

KVLCC2 Tanker. Although data for the total ship resistance C_T is not available for validation, participants submitted predictions at model- and full scale. Of note is the

relatively large scatter in the resistance predictions, particularly at full scale, i.e., the coefficient of variation ($V = 100\bullet$, where σ is the standard deviation) at model- and full scale is 5.2% and 9.3% of the mean predicted value. Prediction and validation of C_T is complicated by the fact that this quantity is obtained from the integration of elemental frictional (viscous) and pressure (inviscid) forces over the hull surface, which have different physics and tend to converge numerically at different rates. As such, both numerical and turbulence modeling errors play important roles in determining the overall accuracy of the resistance prediction. It is speculated that the larger scattered of resistance predictions at full scale is due to the inexperience of grid resolution requirements and the application of turbulence models to full scale flows.

Comparisons of velocity components at the propeller disk plane are used to validate the viscous flow. The KVLCC2 test case shows "hook-shaped" axial velocity contours with low speed fluid at the vortex core due to embedded longitudinal vortices (e.g., Figure 4 of Larsson et al. 2003 and shown here as Figure 2). The predictions from France (ECN/Division Modelisation Numerique, Horus/$r_{ij} - \omega$), USA (FLUENT), Japan (SRI-NEPTUNE and SRI-SURF), Taiwan (USDDC-UVW), and Korea (KRISO-WAVIS) are able to capture this feature with varying degrees of accuracy. It is speculated that the Reynolds stress turbulence models used in the ECN and FLUENT predictions played an important role in this success. However, the successful predictions from Japan are from the Spalart-Allmaras one-equation model, but with a custom-tuned parameter to produce the hook shape. The results from FLUENT and KRISO-WAVIS use wall functions. The last two predictions use a Baldwin-Lomax and realizable $k - \varepsilon$ turbulence model. As expected, results from the two Reynolds stress models produce the most favorable comparisons with turbulent kinetic energy contours.

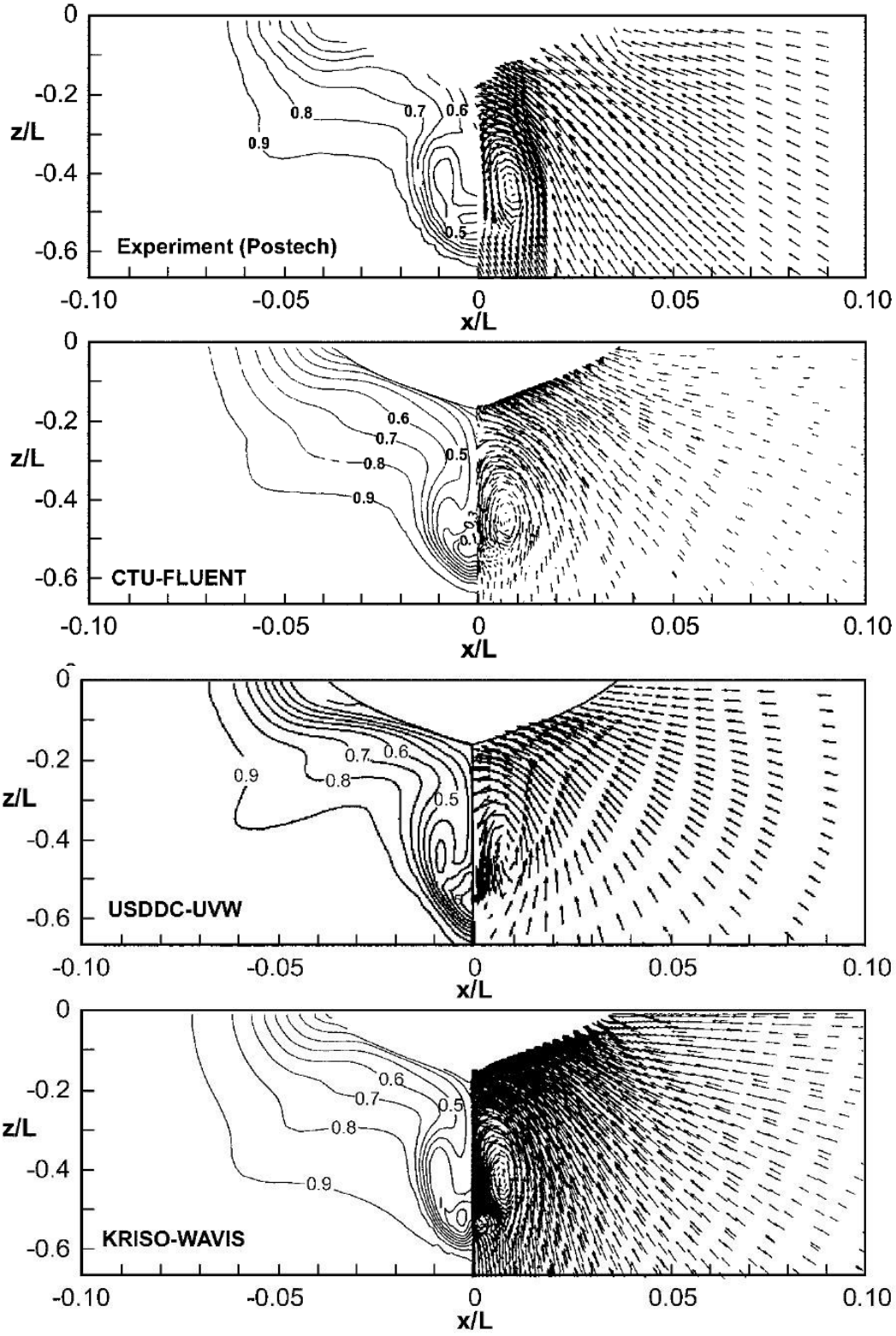

Figure 2 KVLCC2 model scale velocity contours and cross plane vectors at the propeller plane.

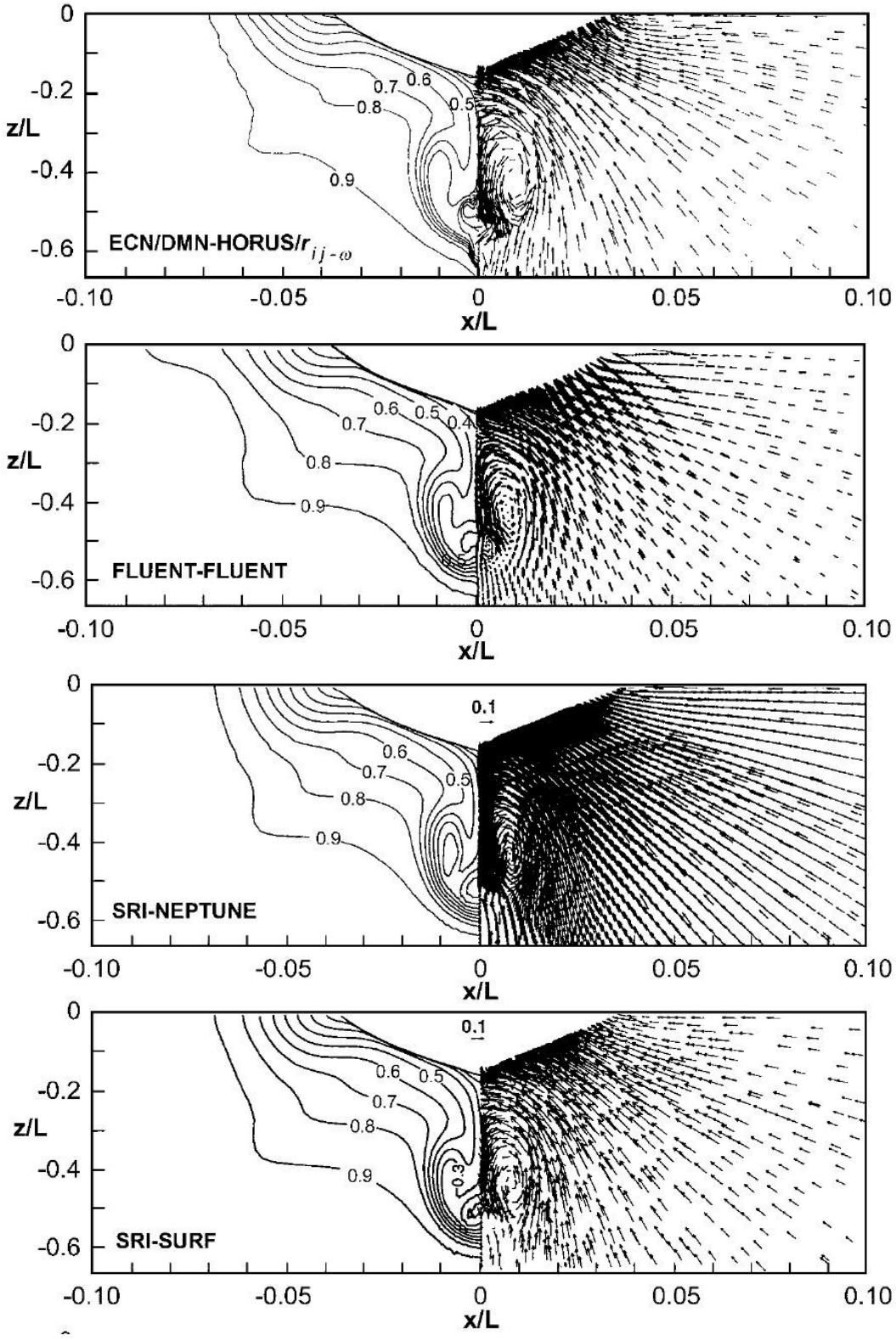

Figure 2 Continued.

KCS Ship. For the unpropelled KCS case, the average comparison difference between resistance predictions and the data is 5.3%, while the scatter of the eight predictions is 5.1%. Seven of the eight predictions were higher than the experimental value with research codes from Finland (HUT-VTT), the Netherlands (MARIN-IST), and Japan (OPU) yielding predictions within 2% of the data. The mean predicted value is 5.0% higher than the data. The two predictions from the commercial codes, COMET (now incorporated into the Star CD code from CD-Adapco Inc.) and CFX, are within 10. 7% and 2.5% of the data, respectively. For the propelled KCS case, two of the three predictions correctly predict an increase in C_T with the addition of the propeller, although no data is available for validation.

Of the six free surface prediction methods, three utilized a surface capturing approach (the computational domain covers both the air and water region) and three a surface tracking approach (the computational domain is dynamically fitted to the free surface and covers the water region only). All methods were able to correctly predict the free surface wave height along the hull with acceptable accuracy, although all underpredicted the wave peak at the bow to some degree, as shown in Figure 10 Larsson et al. (2003) and here as Figure 3. The closest prediction is from the research code HSVA-NEPTUN utilizing a surface capturing approach, which shows roughly a 10% underprediction. Comparison of wave elevation contours away from the hull shows that all solutions, with the exception of that from HSVA-NEPTUN, contain significant dissipation and underprediction of the crests and troughs of the Kelvin wave pattern. Computations from SRI-SURF, using a surface capturing approach similar to HSVA-NEPTUN, show significant dissipation and wave damping in the far-field. Therefore, a consensus on the choice of surface tracking versus capturing is difficult to reach based solely on the G2K results. In practice, predictions are highly dependent of grid density near the free surface and on implementation details of the method. Free surface capturing approaches are required for flows with large amplitude ship motions and maneuvers and/or at higher Froude numbers where steep and overturning waves are generated and surface fitting is not possible. Of the two computations from commercial codes, the HSVA/ICCM-COMET prediction showed one of the most dissipated wave patterns, while the SVA/AEA-CFX group/code did not submit free surface predictions.

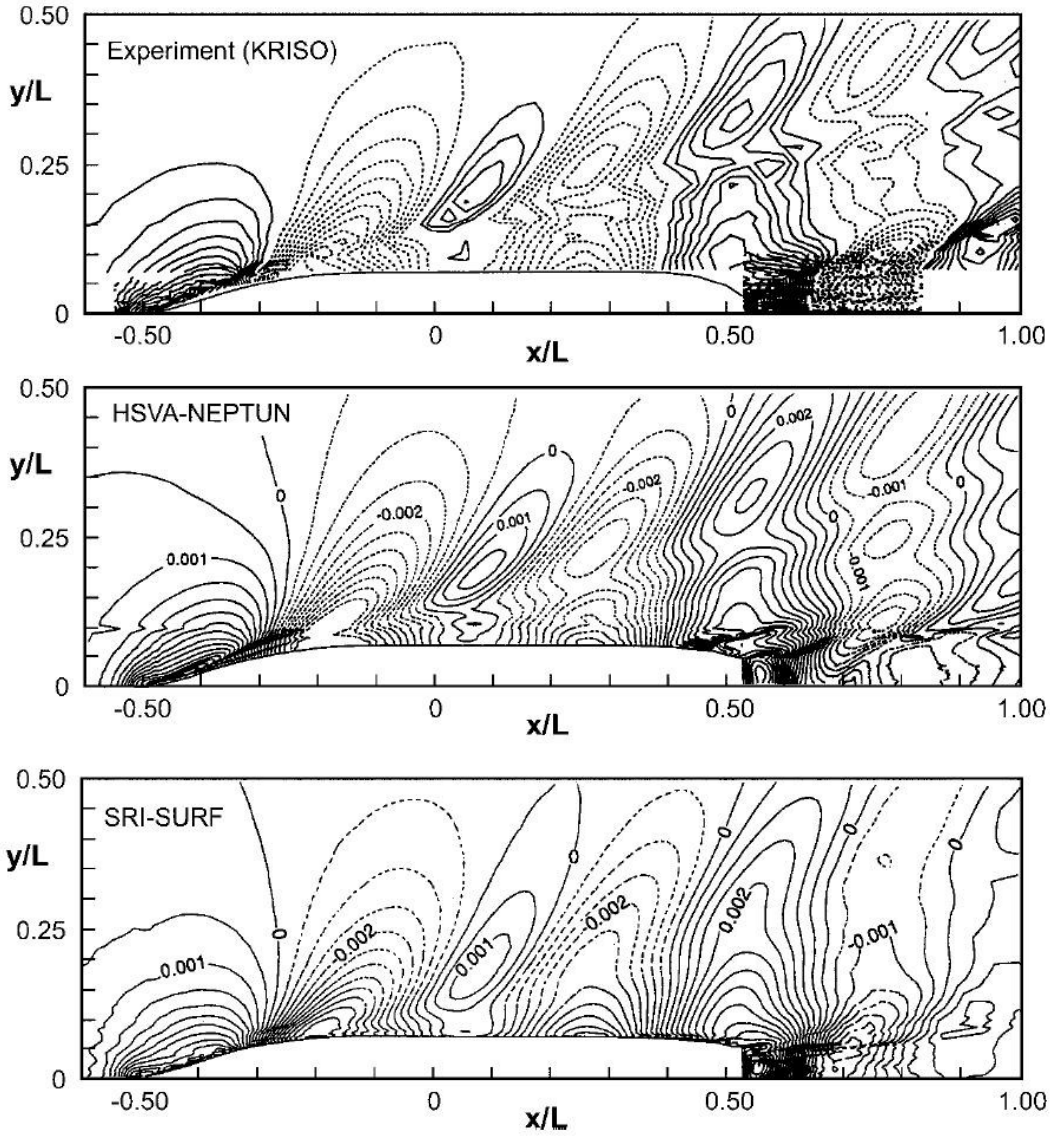

Figure 3 KCS wave elevation contours.

With regard to the viscous flow prediction, the longitudinal vortices strongly affect the velocity contours at the propeller plane, but are considerably weaker than those for the KVLCC2, as shown in Figure 11 Larsson et al. (2003) and here as Figure 4. As a result, the hook-shape is replaced by a thinning of the boundary layer at the center plane and an island of low speed fluid (e.g., Fig 11 of Larsson et al. 2003). Most predictions qualitatively capture this feature with varying degrees of accuracy, with the USDDC-UVW prediction identified as the most favorable. It is noted that a dense grid near the center plane of the propeller disk is required to resolve the small scales of the embedded vortices.

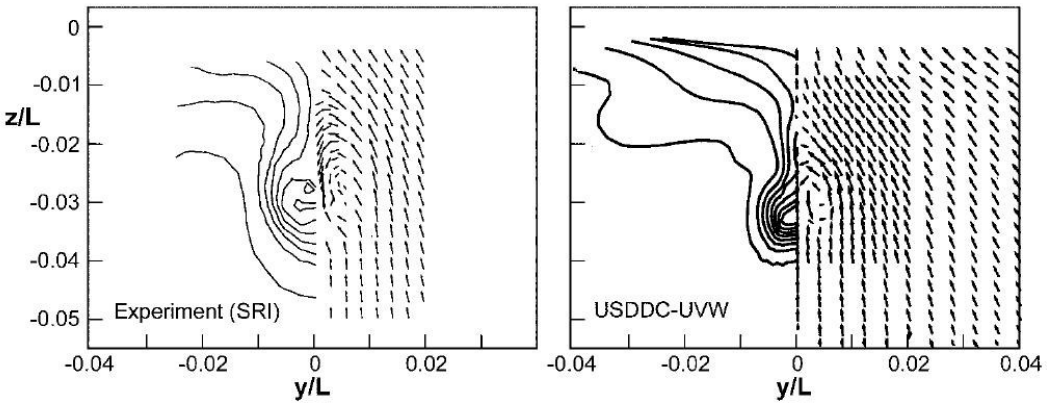

Figure 4 KCS velocity contours and cross-plane vectors at the propeller plane.

DTMB 5415 Surface Combatant. For the DTMB 5415 case, the average comparison error and coefficient of variation from the seven predictions is 4.5% and 4.6%, respectively. The average predicted value is within 0.5% of the data. Four of the seven predictions have comparison errors less than 4%, with the smallest being 3.1%. Predictions from COMET and CFX are within 3.8% and 6.9% of the data, respectively.

Of the six free surface predictions, five use the surface tracking approach, while the lone commercial code COMET uses a volume of fluid surface capturing approach. Comparisons with the data show that most predictions have significant damping of the peaks and troughs of the Kelvin wave system, with the exception of the two surface tracking approaches, INSEAN-MGSHIP and IIHR-CFDSHIP, as shown in Figure 16 Larsson et al. (2003) and here as Figure 5. The commercial code COMET and research code HUT/VTT-FINFLO show rather poor results with highly oscillatory and largely damped wave elevation patterns, respectively. Comparisons with a wave elevation cut measured at a transverse distance of $y/L = 0.172$ from the ship centerline show similar trends, with the INSEAN-MGSHIP prediction displaying excellent agreement and IIHR-CFDSHIP-IOWA showing good agreement. Differences in the amount of dissipation in the far-field wave elevations are partly attributed to grid density in the far-field. Although a direct comparison of free surface grid density is not possible, it should not be surprising that the most well resolved wave patterns from INSEAN-MGSHIP and IIHR-CFDSHIP-IOWA also used the largest grids with 2.6M and 1.8M total grid points, respectively. The average grid size was reported to be 1.3M.

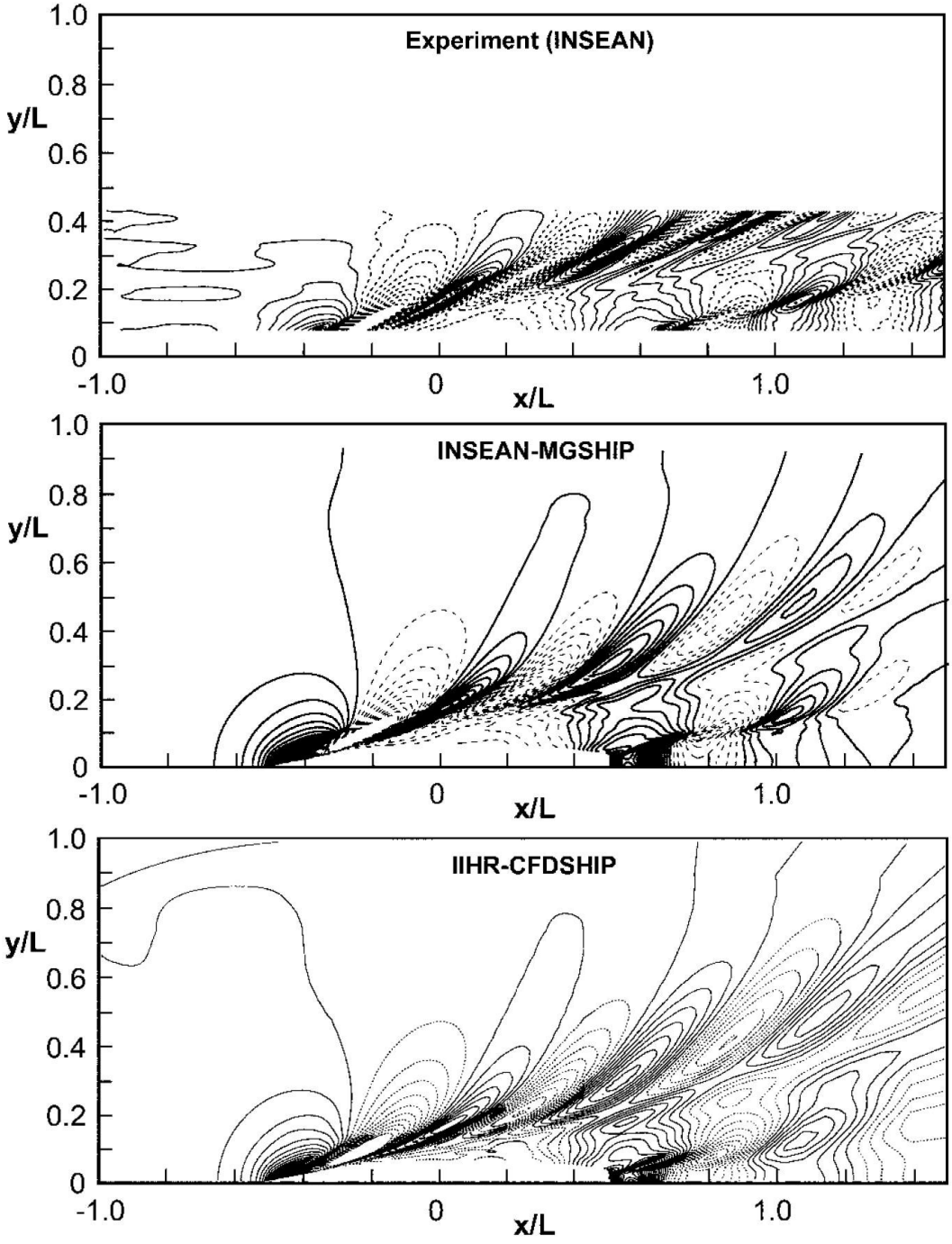

Figure 5 DTMB 5415 wave elevation contours.

Comparison of axial velocity contours and cross flow vectors at the propeller plane, show that roughly half the methods are able to capture the important characteristics of the viscous flow at this location, i.e., the vortex generated at the sonar dome which is convected back to the propeller plan causing a thinning of the boundary layer at the ship

center plane and a "bulge" away from the center plane (e.g., Fig 17 of Larsson et al. 2003). The boundary layers from INSEAN-MGSHIP (Spalart-Allmarus one-equation turbulence model), IIHR-CFDSHIP-IOWA ($k-\omega$ two-equation model), ENC/DHN-ICARE ($k-\omega$), and MSU-UNCLE ($k-\varepsilon$) correctly resolve these features, while those from HUT/VTT-FINFLO (Baldwin-Lomax) and NTU-COMET ($k-\varepsilon$), greatly underpredict the thinning of the boundary layer at the center plane. A comparison of one of the most favorable predictions to the data is shown in Figure 17 Larsson et al. (2003) and here as Figure 6. Successful resolution of these features seems to be largely dependent of grid density and somewhat dependent on turbulence modeling.

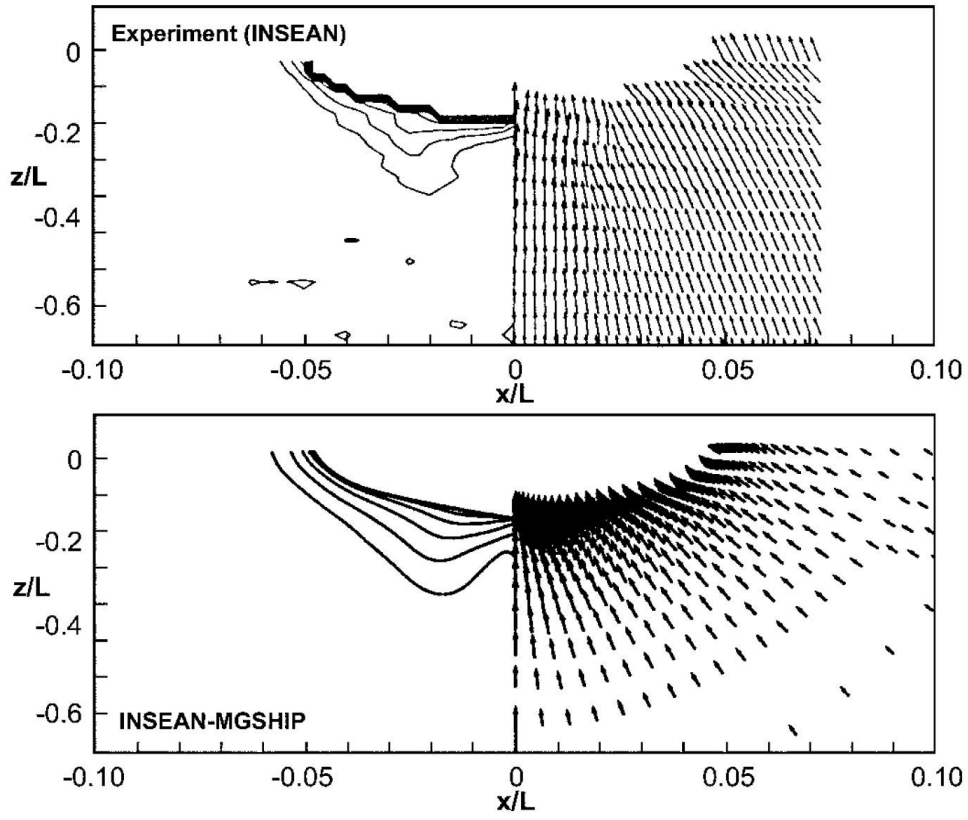

Figure 6 DTMB 5415 velocity contours and cross-plane vectors at the propeller plane.

1.3 CFD Workshop Tokyo 2005

On 9-11 March 2005, the most recent CSH workshop was held in Tokyo, Japan. This workshop was largely a follow-up to the Gothenburg 2000 workshop, with all test

cases and hull forms carried over to the CFD Workshop Tokyo 2005 (CFDWS05), Hino (2005). In this respect, the 2005 workshop allowed the progression of the state-of-the-art in CSH to be assessed. Test cases for the KVLCC2 were added to include steady flow over an obliquely towed model. For the DTMB 5415, test cases were added to predict the (*i*) steady equilibrium ship orientation (i.e., sinkage and trim) and (*ii*) unsteady flow for forward speed diffraction with incident waves. Also, a set of 5 common grids were generated and made available for the KVLCC2 geometry, so that the uncertainty of varying grid density would be eliminated for this test case. A detailed explanation of test case conditions can be found at the URL: http://www.nmri.go.jp/cfd/cfdws05. For CFDWS05, a total of 20 groups participated, from 13 countries using 14 research codes and 3 commercial codes (i.e., Fluent, Comet, and CFX).

KVLCC2 Tanker. Thirteen predictions of model scale ship resistance were submitted for the straight-ahead test case. Although no data is available for validation, the prediction scatter is even higher than the previous workshop (V = 6.9% compared to 5.2% for G2K). The scatter for the obliquely towed case is 9.4%, 10.1%, 9.7%, and 10.5% for oblique tow angles of 0, 3, 6, and 9 degrees, respectively.

Examination of axial velocity contours at the propeller plane for the straight-ahead condition shows similar trends as those described above for the G2K workshop; computations using Reynolds stress (RS) turbulence models and other models that are calibrated for these flows show better agreement with measurements in predicting the hook feature. Results from the ECN/CNRS-ISIS (4 variants of RS), SOTON-CFX5 (RS), KRISO-WAVIS (two-equation), and USDDC-UVW (Baldwin Lomax) codes show the closest agreement. Axial velocity contours from 11 predictions are compared with data in Figure 7 for the 12 degree obliquely towed case.

For the obliquely towed case, 16 predictions were submitted for longitudinal force C_X, lateral force C_Y, and turning moment C_N coefficients over a range of towing angles from 0 to 15 degrees, with almost all codes showing a very reasonable level of agreement with the data. Most all codes showed insensitivity of C_X to tow angle in accordance with data, with the exception of the USDDC-UVW and NSWC-UNCLE RS results which underpredict C_X. The correct trends for C_Y and C_N versus towing angle are reproduced

by all results, with the largest discrepancy in the predictions occurring at the two largest tow angles of 9 and 12 degrees. The closest agreement for C_Y and C_N quantities appears to be the FLUENT-FLUENT and ECN/CNRS-ISIS predictions.

KCS Ship. In comparison to the G2K workshop results, the mean value of the 11 predictions (all from research codes) is just 1.1% higher than the data, compared with a value of 5% for the G2K workshop. The prediction scatter is also smaller at 4.2% compared to the previous workshop value of 5.1%. Predictions from FINLAND-CFDFLOW, ECN/CNRS-ISIS, KRISO-WAVIS, OPU-FLOWPAC, and USDDC-UVW are within 2% of the data. In contrast with the previous workshop, most all methods are able to resolve the Kelvin wave pattern with a reasonably small level of far-field dissipation. Predictions with higher levels of dissipation include those from OPU-FLOWPACK, OPU-CFDSHIP-IOWA, and NMRI-SURF. Comparison of axial velocity contours and cross flow vectors at the propeller plane show that, like the previous workshop, most all methods predict the thinning of the boundary layer near the center plane and island of low speed fluid. For the self-propelled case, the overall level of agreement in the propeller wake is reasonable and the change in the pressure field correlates well with the measurements.

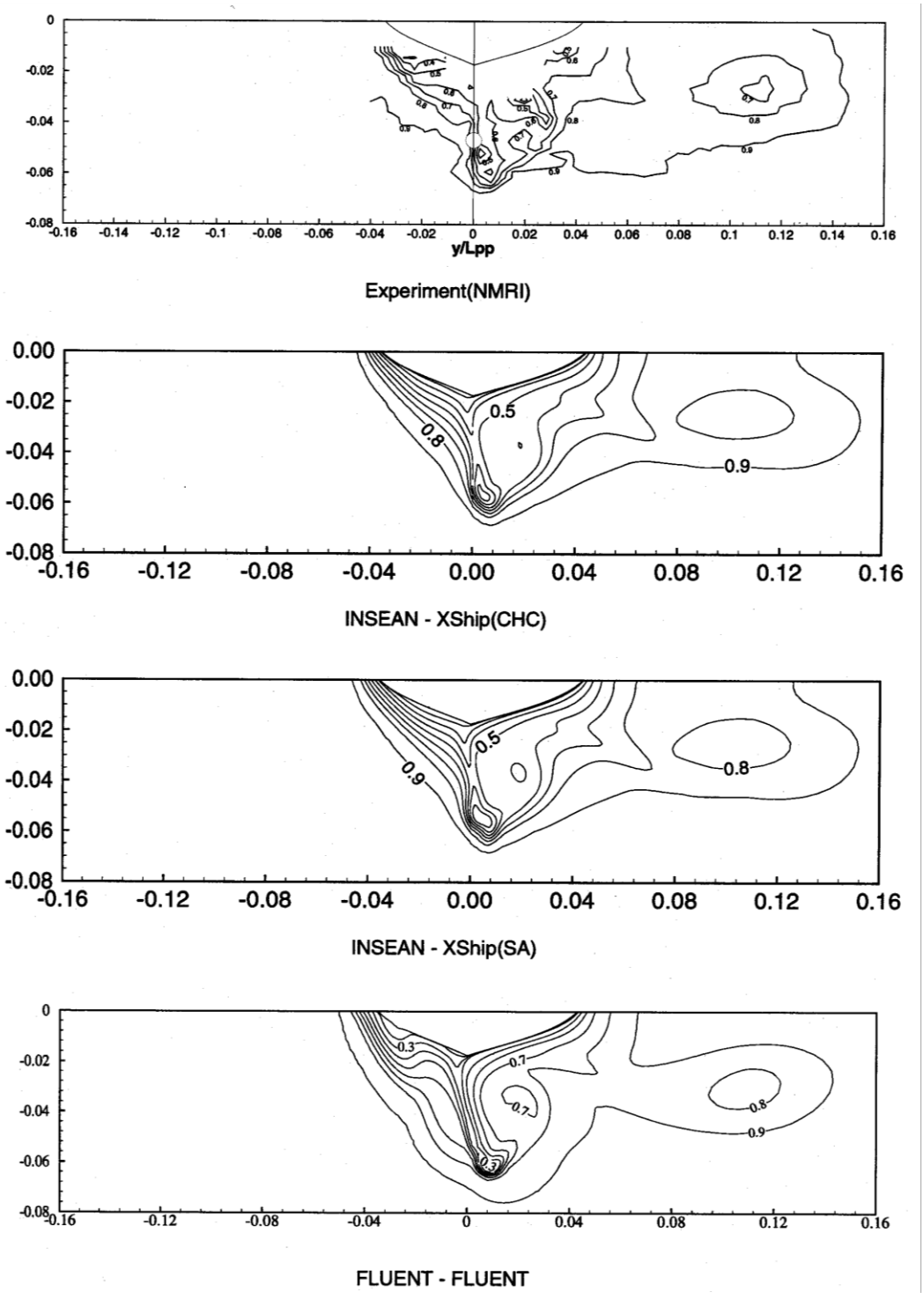

Figure 7 KVLCC2 model scale velocity contours at the propeller plane for the obliquely towed case (12 degrees).

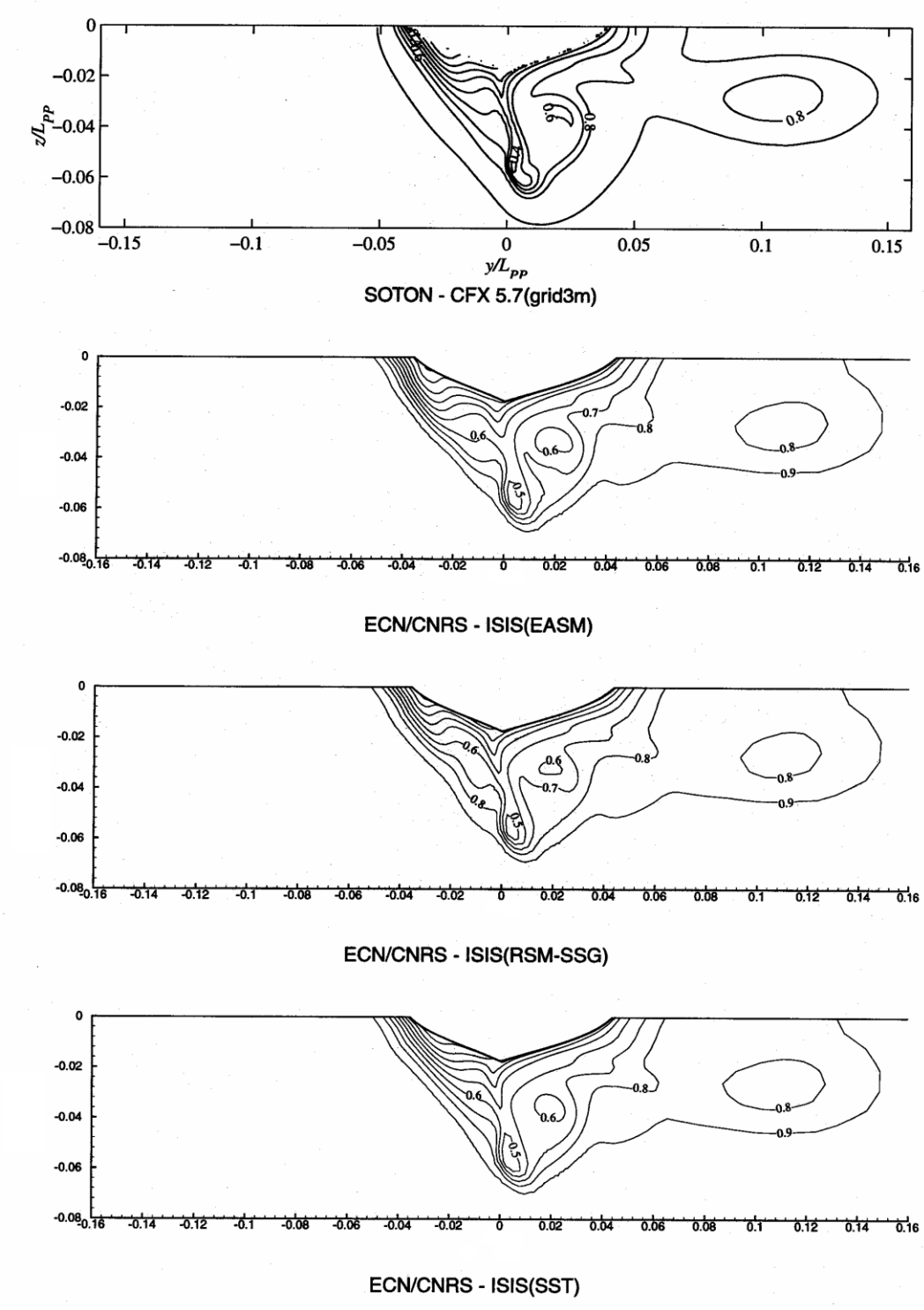

Figure 7 Continued.

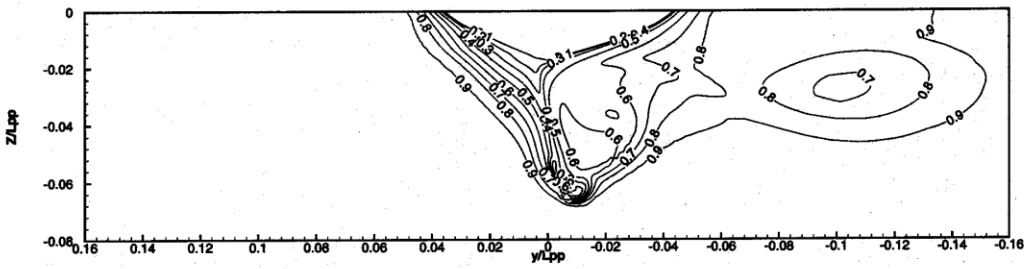

NSWC - UNCLE(qo)

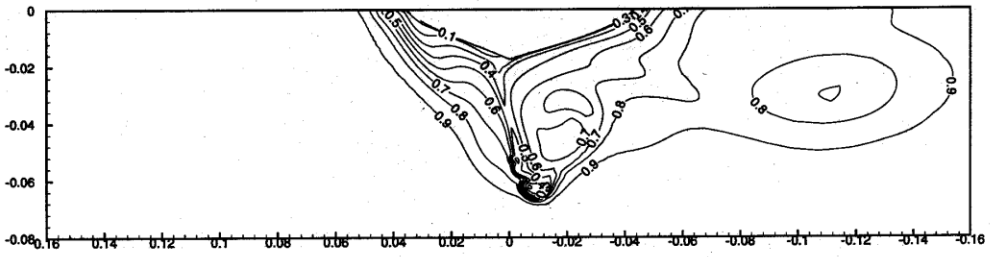

NSWC - UNCLE(rsm)

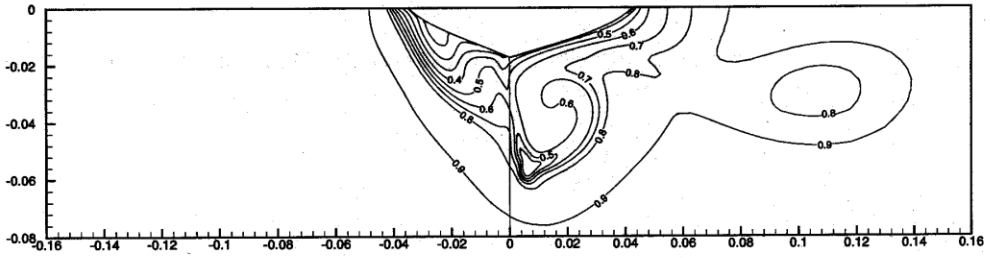

KRISO - WAVIS

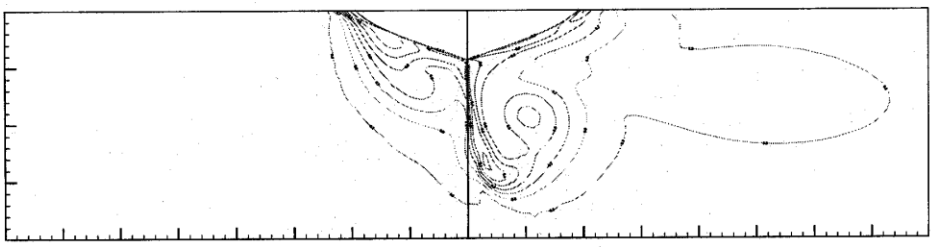

USDDC - UVW

Figure 7 Continued.

DTMB 5415 Surface Combatant. For the steady test case in calm water, resistance predictions from nine research and two commercial codes yield a comparison difference between the mean prediction and measurement of only 0.17% compared with the previous workshop value of 0.5%. However, in comparison with the previous workshop, the scatter in the predictions is much higher at 7.1% compared to 4.6%. The two commercial codes, FLUENT and COMET, underpredict resistance by 9.46% and 1.9%, respectively. Comparison of the free surface predictions again shows much better resolution of the far-field waves in comparison to calculations of the G2K workshop. Exceptions to this trend are seen in the results of CYCU-COMET and MARIN-PARNASSOS which contain unphysical high-frequency waves and in the ECN/BEC-ICARE result which shows large wave dissipation in the far-field.

Steady axial velocity contours and cross plane vectors from 10 of the 11 predictions show correct thinning of the boundary layer at the center plane and the off center plane bulge, with varying degrees of accuracy. The USDDC-UVW result shows an incorrect boundary layer prediction with maximum thickness at the center plane.

For the forward speed diffraction test case with incident waves, prediction of the mean and first harmonic amplitudes of the unsteady free surface and boundary layer at the propeller plane are compared with measurements. Overall, the mean and first harmonic wave amplitudes from the four predictions show good agreement with the data, although the result from ECN/BEC-ICARE shows greater dissipation for both quantities. A comparison of one of the better submissions (CFDSHIP-IOWA) is provided for a quarter-phase sequence of wave elevations in Figure 8 and Figure 9 and for axial velocity contours in Figure 10 and Figure 11.

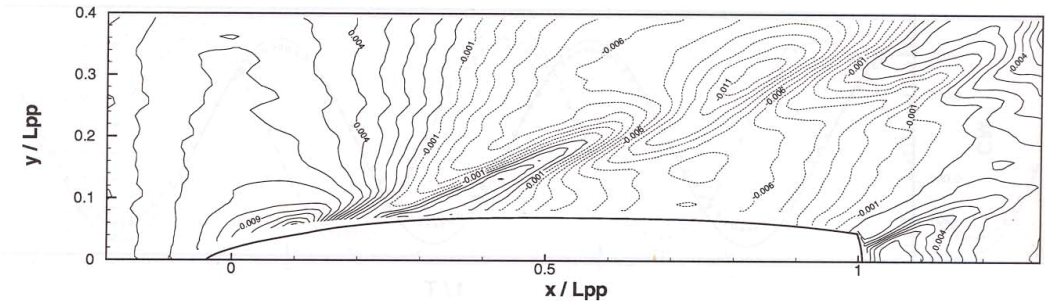

$t/T_e = 0/4$

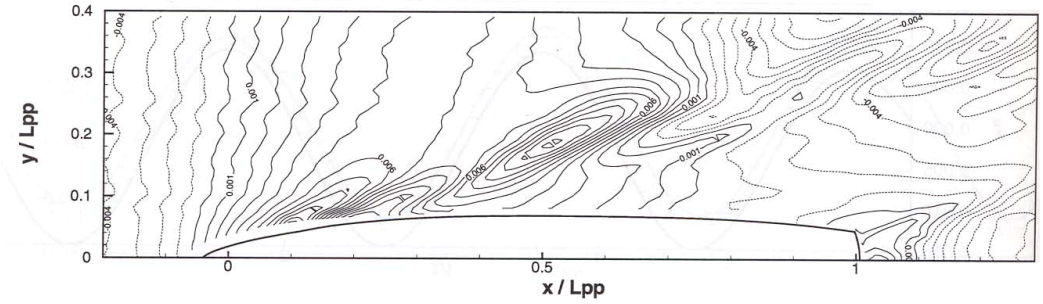

$t/T_e = 1/4$

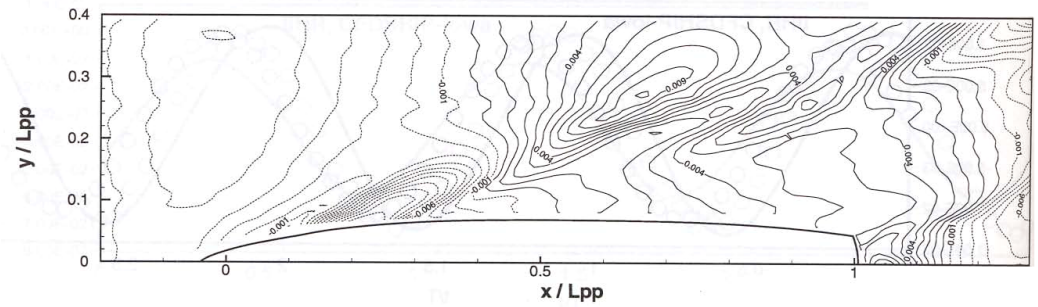

$t/T_e = 2/4$

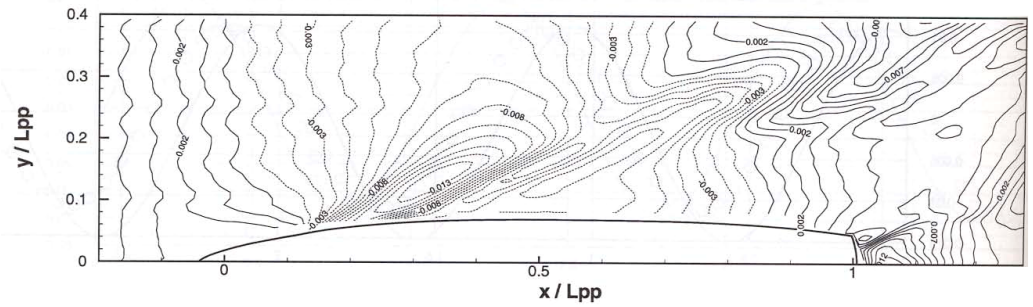

$t/T_e = 3/4$

Figure 8 Measurements for quarter phase sequence of wave elevation contours: DTMB 5415 forward speed diffraction case.

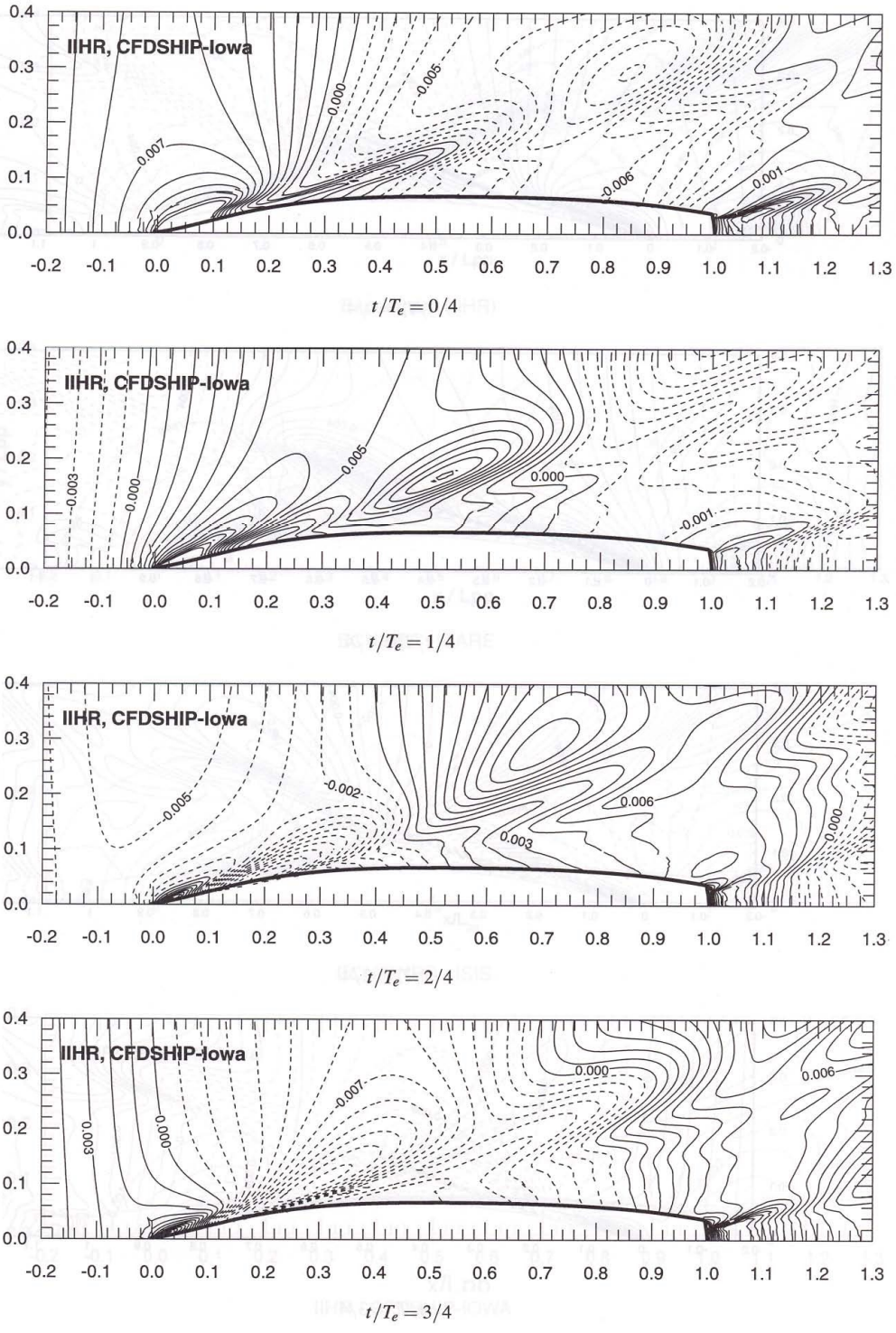

Figure 9 Prediction for quarter phase sequence of wave elevation contours: DTMB 5415 forward speed diffraction case.

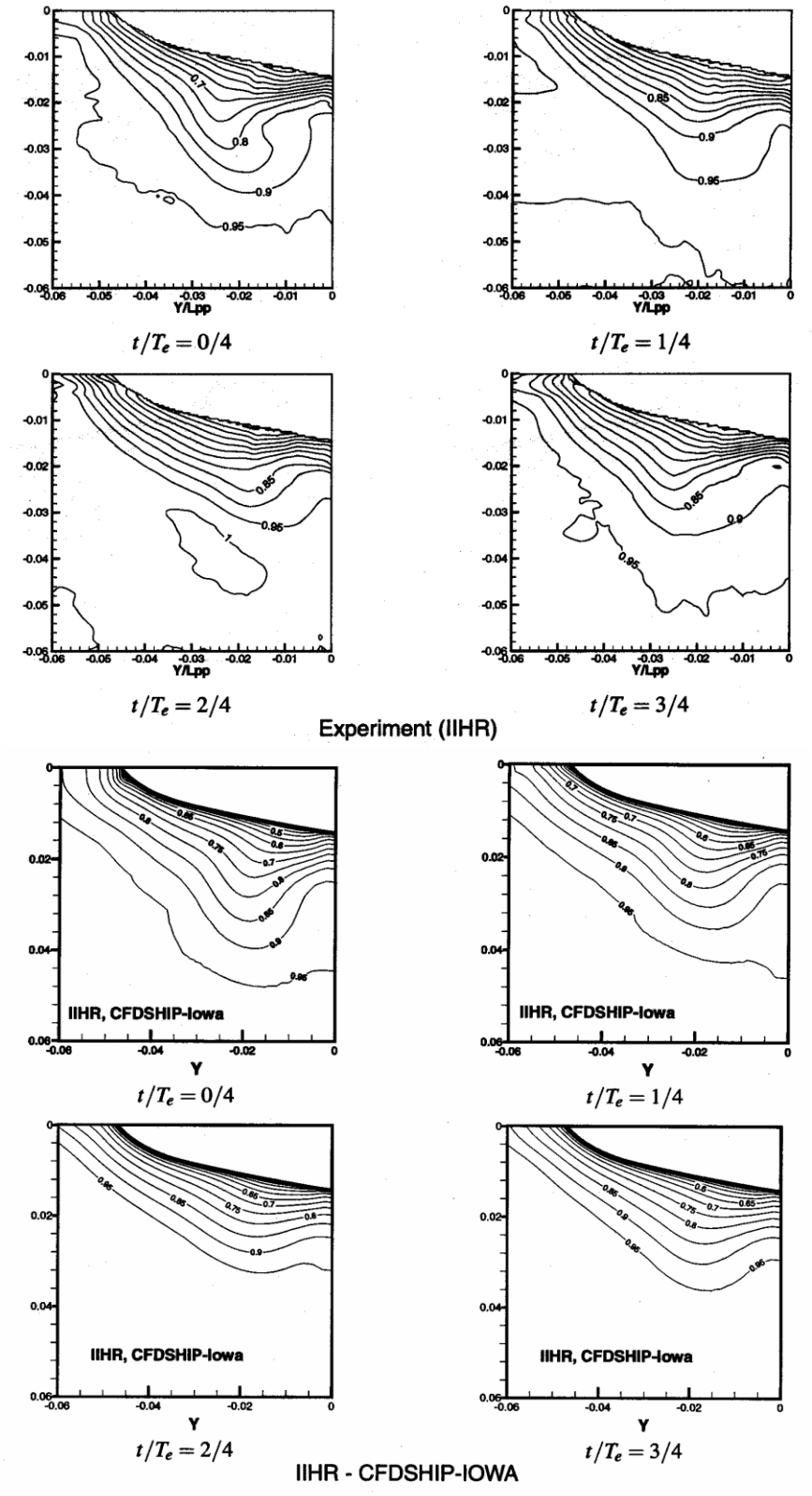

Figure 10 Measurements (top) and prediction (bottom) for axial velocity contours: DTMB 5415 forward speed diffraction case.

Comparison of the CFDWS05 predictions with those from the G2K workshop shows that a majority of participants used research codes for test case computations. Results from the commercial codes of Fluent, Comet, and CFX were also submitted. The prediction of resistance coefficients for the KCS and DTMB 5415 hulls was slightly improved, but the prediction scatter was larger for the KVLCC and DTMB 5415 hulls. With regard to the free surface predictions, the resolution of the Kelvin wave pattern was in general much improved due to the use of finer grids and improved numerical solution techniques. For prediction of boundary layers with embedded longitudinal vortices, the results from Reynolds stress turbulence models appear to be better than those from zero-, one-, and two-equation models. In addition, adequate grid resolution is required to capture the small scales of the vortex core.

1.4 Current Status

Although past workshops on the application of RANS methods to CSH have focused mainly on steady free surface flow for resistance and powering, such approaches are now being applied to (*i*) the ship motion response to ocean waves and (*ii*) desired change in ship course due to deflection of control surfaces, known as seakeeping and maneuvering, respectively. Examples of RANS applications to seakeeping in the literature can be found in Hochbaum and Vogt (2002), Orihara and Miyata (2003), Carrica et al. (2007b), and Wilson et al. (2006b), while applications for unsteady maneuvering can be found in Hochbaum (2006), Wilson et al. (2007b), and Di Mascio et al. (2006), as shown in Figure 11. Recently, a workshop on ship maneuvering was held in Copenhagen, Denmark on 14-16 April 2008 (SIMMAN: Workshop on Verification and Validation of Ship Maneuvering Simulation Methods, http://www.simman2008.dk/). Test cases included planar motion mechanism, captive model, and free model maneuvering predictions for the KVLCC, KCS, and DTMB 5415 ship hulls. Workshop proceedings will be available in late 2008.

Surface capturing techniques are now the preferred approach for free surface modeling and are required to manage steep, overturning, and breaking waves associated with high Froude number, large amplitude motions and maneuvering, and high sea states. Di Mascio et al. (2007) and Wilson et al. (2007a) have used the single phase level set to

simulate breaking waves over the DTMB 5415 at higher Froude number. Others have used multi-phase volume-of-fluid methods to manage complex free surface topologies, e.g., Visonneau et al (2006), Wilson et al. (2006c), and Maki et al. (2006).

On 4 April 2005, the Office of Naval Research (ONR) held a closed forum workshop to assess the ability of ONR-supported CFD codes to predict bow and transom wave breaking for high-speed ships. Predictions of resistance and free surface wave patterns were submitted in a blind fashion by four groups using five CFD codes as discussed in Wilson et al. (2006d). A mix of research [CFDSHIP-IOWA (RANS), NFA (Cartesian solver with body force no-slip boundary condition), Das Boot (potential flow)] and commercial [Fluent (RANS) and Comet (RANS)] codes were used and the physical and numerical modeling, accuracy, gridding strategy, and ease of use were discussed. Both the research and commercial RANS codes were able to resolve the breaking waves to varying degrees of fidelity largely dependent on the localized grid density used, with typical grid counts on the order of several million points. Figure 12 shows a comparison of predictions for stern wave breaking at $Fr = 0.43$. The Cartesian solver used an order of magnitude more total grid points. As a result, the NFA prediction was able to resolve small scale details of the wave breaking. However, the body force boundary condition did not allow the turbulent boundary layer to be resolved so that accurate prediction of the frictional force was not possible.

Computational ship hydrodynamics presents unique challenges for grid generation due to turbulent boundary layer and free surface resolution requirements, complex geometry such as fully appended ships, and large amplitude motions and incident waves. Traditional approaches to gridding complex ship geometries include body-fitted structured grids, which can be tedious, time consuming and require a non-trivial level of expertise. Some flexibility can be added through the use of overset grids, where overlapping blocks can be locally generated around each appendage or used for local grid refinement. Grid connectivity and interpolation stencils are generated in a pre-processing step or dynamically during the flow solution, as discussed in Noack (2007) and shown in Figure 13 for a fully appended ship. Carrica et al. (2006) used dynamic overset grids for the R/V Athena fully appended geometry, where the ship orientation and body-fitted grid were adjusted to achieve dynamic equilibrium over a range of speeds, while the

background block remained fixed. Overset grids for local refinement of breaking bow and stern waves were used for the R/V Athena patrol boat (Wilson et al., 2006a) and for a surface combatant (Wilson et al., 2007a).

Mixed-element, body-fitted unstructured approaches have also been used to manage complex ship geometries. Typically, prism layers must be used to achieve near-wall spacing requirements for turbulence modeling and to avoid high-aspect ratio, poor quality tetrahedral cells near the no-slip surface. Application of unstructured approaches have been given for design of podded propulsors (Hino, 2006), an offloading vessel in waves (Yang et al., 2007), a surface combatant with planar motion mechanism maneuvers (Wilson et al., 2007b), and a high-speed trimaran (Maki et al., 2007) as shown in Figure 13. Another motivation for the use of unstructured grids is in local mesh refinement, where it is much easier to locally insert grid points to an existing mesh. Hay and Visonneau (2005) reported RANS computations using an unstructured solver for free surface flows over the Series 60 cargo ship in drift and the Wigley hull with grid adaption to the free surface.

Due to the labor involved in generating traditional body-fitted structured or unstructured grids, Cartesian grid generation techniques have received increased interest. Dommermuth et al. (2007) presented Euler calculations on highly refined Cartesian grids using a volume of fluids free surface model and an immersed-boundary approach to simulate breaking waves for the Athena patrol boat geometry as displayed in Figure 14. Yang et al. (2007) presented preliminary results using Cartesian grids where no-slip boundary conditions were fixed from a previous viscous solution on a body-fitted curvilinear grid. Karman and Wilson (2008) presented a Cartesian-based approach which uses an octree refinement with general cutting to create hybrid meshes. Viscous prism layers are inserted using linear-elastic elliptic smoothing. Adaptive refinement was used to increase the resolution of pertinent flow features, such as the air-water interface and vortical flow features in the solution.

Linear one- and two-equation eddy viscosity turbulence models are by far the most widely used models, as apparent from the previously discussed review of the CSH workshops. Recently, both large-eddy simulation (LES) and hybrid RANS/LES

approaches have been used for both academic and practical test cases to overcome deficiencies in isotropic eddy viscosity turbulence models. Bensow et al. (2006) investigated flows neglecting the free surface for a 3D hill and an axisymmetric submarine model (DARPA suboff) using RANS, LES, and hybrid RANS/LES approaches. Kim and Cokljat (2007) used a developmental version of the commercial code Fluent to perform both LES and DES simulations for a free surface piercing hydrofoil and circular cylinder. They reported that the DES approach was able to capture complex features of turbulent free surface flows such as spilling-breaking bow waves, shoulder waves, flow separation, and bubble formation. Also, they found that the quality of the LES degrades quickly as the mesh becomes too coarse to capture the Kelvin wave pattern. Xing et al. (2007) performed isotropic and Reynolds stress RANS and DES calculations over the KVLCC2 at large drift angles and by neglecting the free surface using CFDSHIP-IOWA. As expected, the RANS calculation using the Reynolds stress model yielded better prediction of the resistance coefficient, axial velocity, and turbulent kinetic energy for drift angles of 0 and 12 degrees. At larger drift angles of 30 and 60 degrees, the flow becomes unsteady and the DES approach was used.

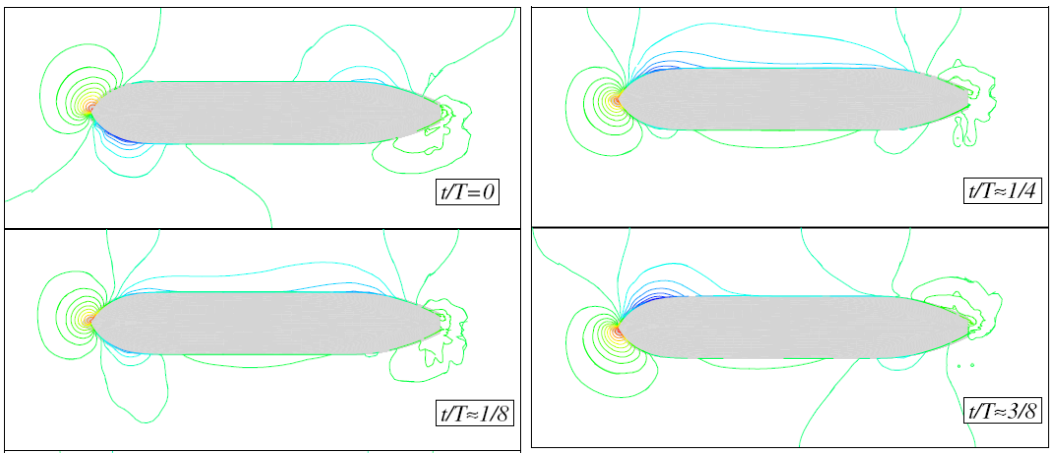

Figure 11 Wave contours for KVLCC2 pure sway maneuver in a narrow basin from DiMascio et al (2006) .

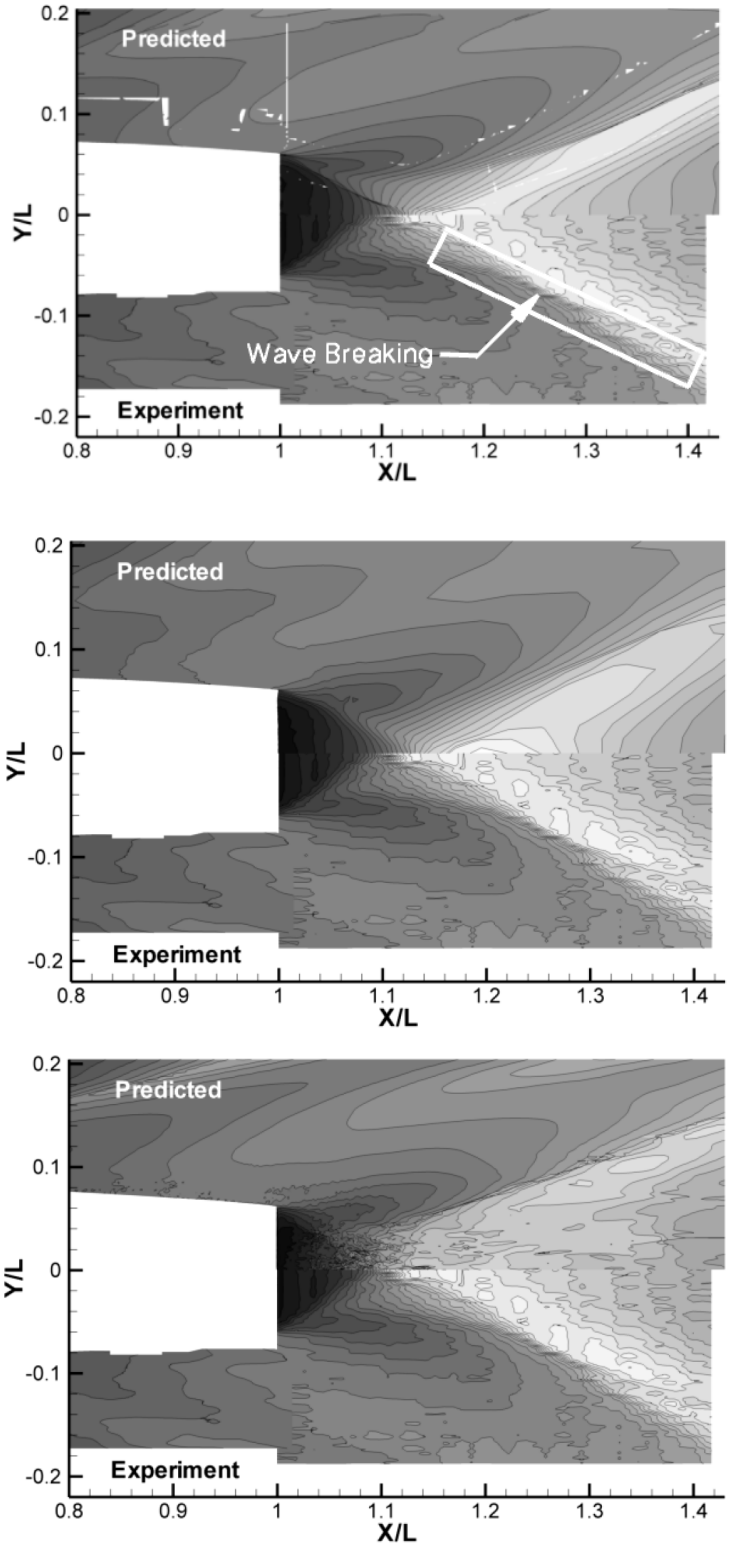

Figure 12 Prediction of stern wave breaking for the Athena ship: CFDSHIP-IOWA (top), COMET (middle), and NFA (bottom) from Wilson et al. (2006d).

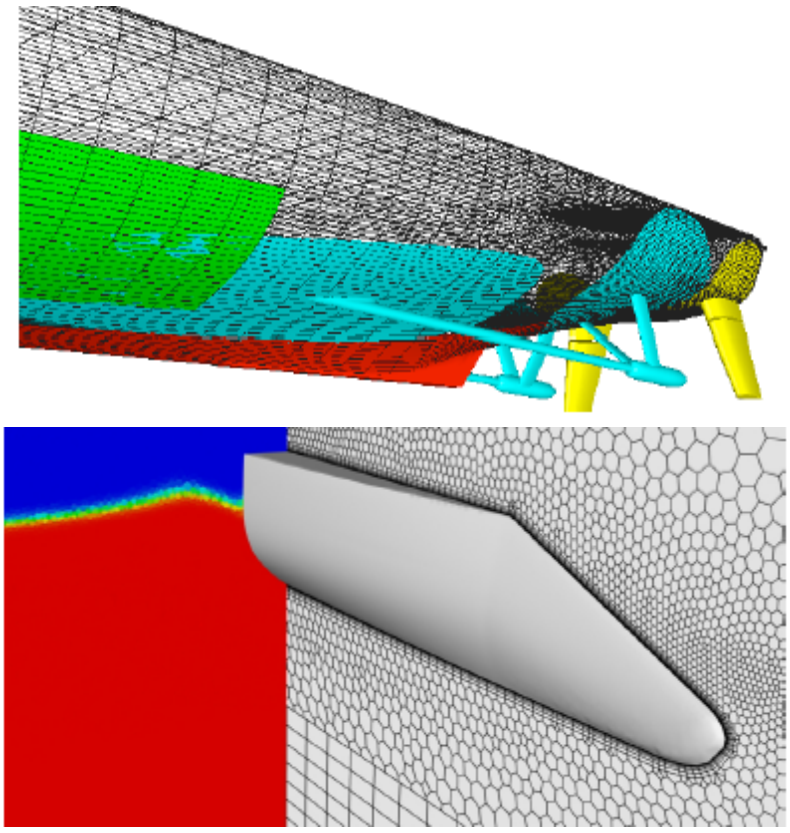

Figure 13 Structured overset (Noack, 2007: top)
and unstructured mixed element (Maki et al., 2007: bottom) grids.

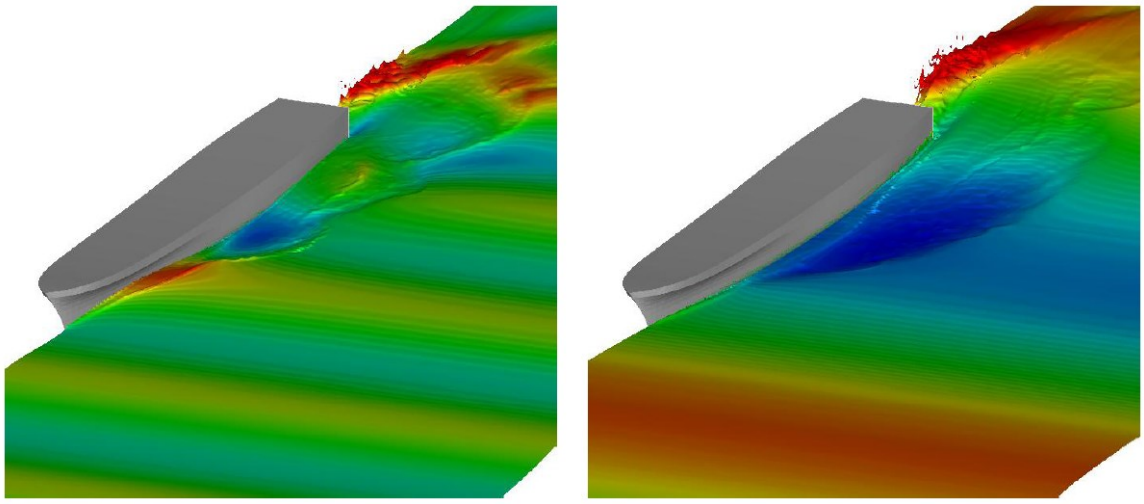

Figure 14 Wave elevation contours for R/V Athena in regular waves using Cartesian/immersed boundary method.with $\lambda = L/2$ (left) and $\lambda = L$ (right) from Dommermuth et al. (2007).

2 CFDSHIP-IOWA and TENASI RANS codes

2.1 CFDSHIP-IOWA

CFDSHIP-IOWA is a general purpose parallel unsteady RANS research code with free surface capability developed at the University of Iowa, IIHR – Hydroscience and Engineering Laboratory over the past 15 years. The code solves the incompressible Navier-Stokes equations in an inertial coordinate system. A single phase level set approach is used to model the free surface, where a transport equation defines the air/water interface as the zero iso-level of a scalar function (Carrica et al., 2007a). The computational domain encompasses both the air and water region, with the Navier-Stokes equations enforced in the water region while the points in air are used to satisfy the dynamic free surface boundary conditions at the interface. The turbulent kinetic energy is typically computed using a blended $k-\varepsilon/k-\omega$ model (Menter, 1994), although Reynolds stress and detached eddy simulation models have also been used for ship flows (Xing et al., 2007).

The governing equations are transformed from the physical domain to the orthogonal computational domain resulting in a structured multi-block body-fitted approach. The convective terms are discretized using higher-order upwind biased schemes, while diffusion terms are discretized using a standard second-order method. Temporal discretization is accomplished using an implicit three-level, second-order accurate Euler scheme. The momentum equations are solved in a sequential fashion using alternating direction implicit line sweeps. The incompressibility condition is enforced using the PISO algorithm, which results in a discrete pressure-Poission equation. This equation is solved using preconditioned Krylov solvers available in the PETSc package (Balay et al. 2002). Propellers can be modeled in CFDSHIP-IOWA through a prescribed axisymmetric body force approach. Both regular and irregular waves can be modeled by specifying time dependent inflow boundary conditions based on a superposition of linear potential flow solutions for surface gravity waves (Carrica et al., 2008).

A hierarchical range of ship motions can be predicted in CFDSHIP-IOWA by integration of the 6DOF equations of motion. The motions are described by translations

with respect to the initial static location of the center of gravity in the earth fixed frame and by Euler angles which define the ship rotations. The 6DOF equations are integrated using a predictor-corrector iterative approach. The predictor step is explicit in nature and uses the resultant ship forces and moments at the past time step to approximate the current ship orientation at the new current time. In the corrector step, the most up to date iterates of forces and moments are used in the integration of the 6DOF equations.

For complex ship geometries and relative body motions, CFDSHIP-IOWA has a dynamic overset gridding capability. The outer fringe points of the overset embedded blocks are treated as boundary conditions which are computed by interpolation of the flow field from donor blocks. The domain connectivity and interpolation stencils can be computed in a pre-processing step (static) or through concurrently executed software at the beginning of each time step during the flow solution. The software package, SUGGAR is used to manage the overset operations (Noack, 2005).

Capability for simulation of breaking waves with CFDSHIP-IOWA has been reported in Wilson et al. (2006a) for the R/V Athena and Wilson et al. (2007a) for a surface combatant as shown in Figure 15. Prediction of large amplitude ship motions with incident waves was shown in Carrica et al. (2006) and Carrica et al. (2007b) for a leading-following two ship configuration (Figure 16), while simulation of unsteady ship maneuvers was shown in Carrica et al. (2006) (Figure 17). A comparison of RANS solutions with Reynolds stress closure models and DES for the KVLCC2 geometry was given by Xing et al. (2007). Paik et al. (2008) applied CFDSHIP-IOWA to the solution of the fluid-structure hydroelastic problem by predicting ship motions for the S175 container ship with incident waves. The time-dependent hull forces and moments from the solution were then transferred to the University of Michigan structural analysis group, which predicted the dynamic structural response of the hull to the incident waves. The numerical optimization of a fast catamaran using CFDSHIP-IOWA was presented in Tahara et al. (2007).

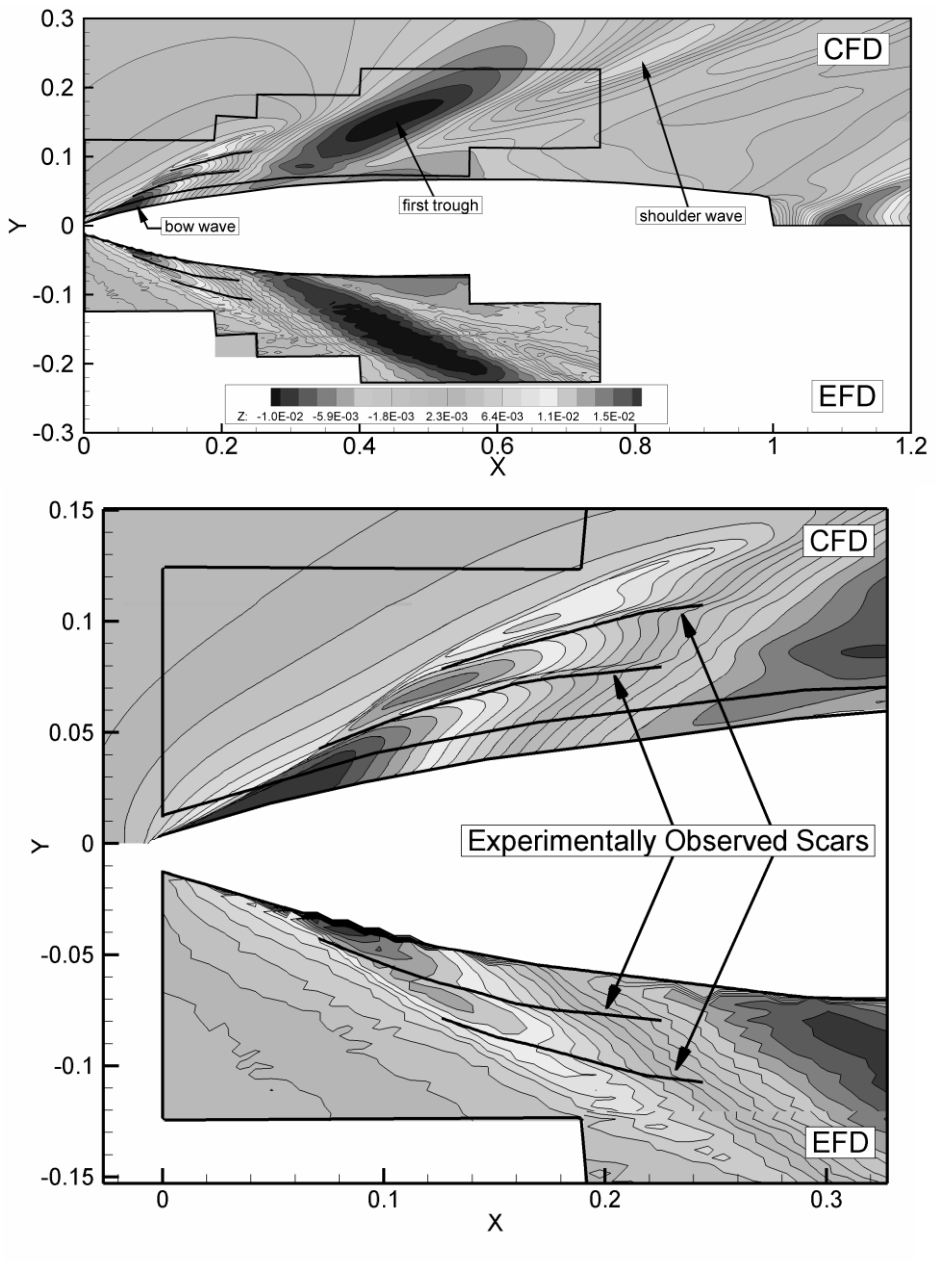

Figure 15 Comparison of CFD solution and EFD measurements for 5415 wave breaking: wave contours (top) and bow wave details (bottom), *Fr*=0.35 from Wilson et al. (2007a).

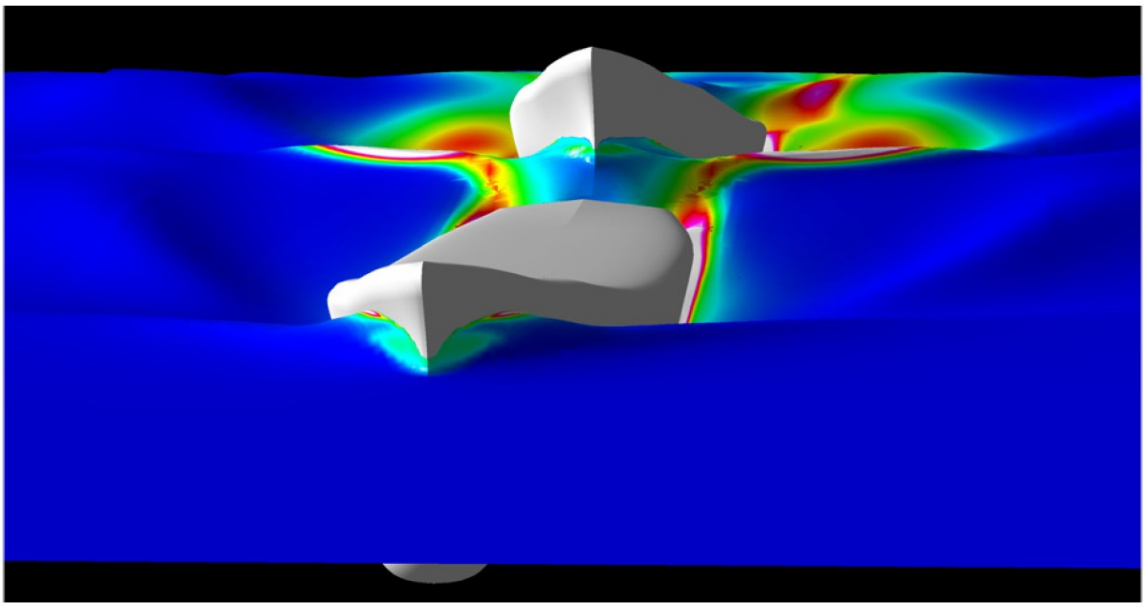

Figure 16 Free surface prediction for 5415
two ship configuration from Carrica et al. (2006).

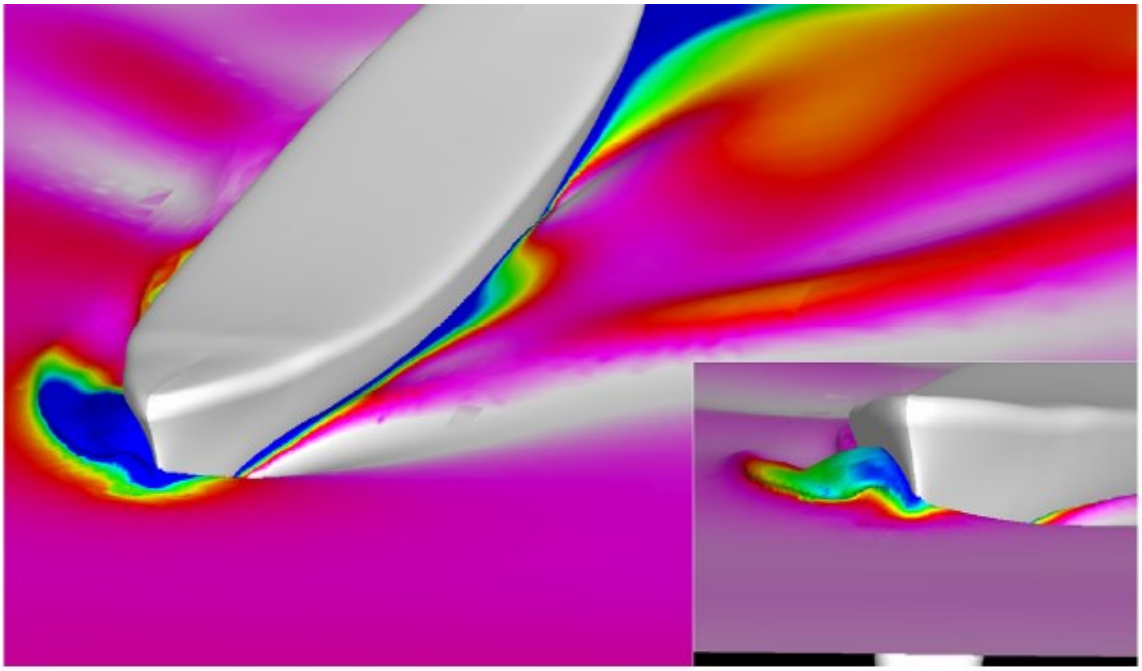

Figure 17 Free surface prediction for 5415 with a
pure sway maneuver from Carrica et al. (2006).

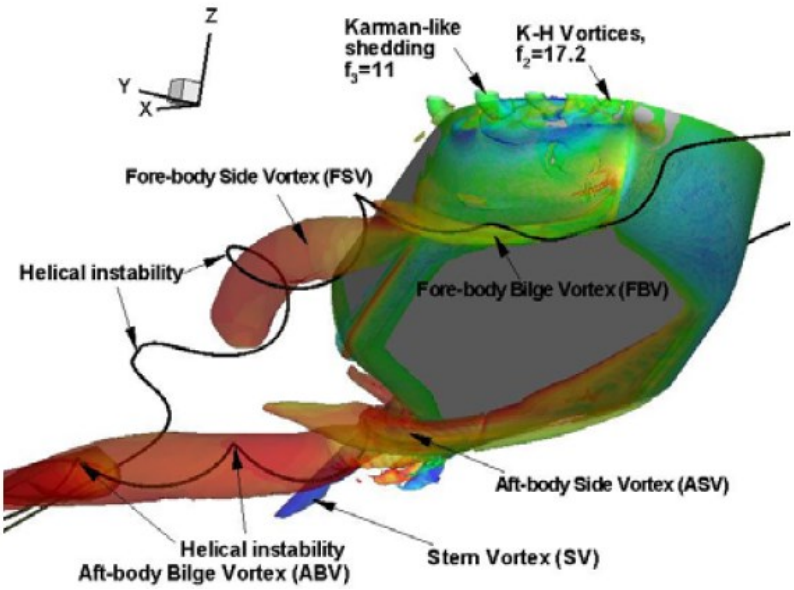

Figure 18 Vortex system from DES simulation of KVLCC2 at 30 degree drift angle from Xing et al. (2007).

2.2 TENASI

The core algorithm utilized is related to several previous efforts and has evolved over more than 15 years, initially at the NSF ERC, Mississippi State University as the UNCLE code and then later at the SimCenter: National Center for Computational Engineering, The University of Tennessee at Chattanooga from 2002 to the present as the Tenasi code. The approach is an evolution of the implicit flow solver and code of Anderson et al. (Anderson, 1992; Anderson and Bonhaus, 1994; Anderson et al., 1995). The solver developed in these studies demonstrated 3D, implicit, high Reynolds number solution capability. Aspects of the present approach are also related to the parallel multiblock structured grid solver of Pankajakshan and Briley (1995); the parallel version of the unstructured algorithm is detailed in Hyams (2000). The approach has also been applied to naval hydrodynamic applications using the UNCLE code in Hyams et al. (2000).

The general-purpose parallel-unstructured viscous flow solver, Tenasi, developed at the SimCenter: National Center for Computational Engineering, The University of

Tennessee at Chattanooga, is used to simulate free surface flow over practical ship geometries. The current unstructured algorithm solves the RANS equations with a general *N*-faced polyhedral element type. A multiphase free-surface capturing technique is implemented to overcome limitations associated with surface tracking/fitting approaches and to manage complex interfacial topologies such as steep and overturning waves associated with high Froude number and/or large amplitude ship motions and maneuvers (Nichols, 2002). The non-dimensional incompressible continuity in pseudo-compressibility form, RANS momentum equations, and non-conservative transport of the liquid volume fraction are solved in primitive variable form in a fully-coupled 5 *x* 5 block matrix approach. The volume fraction is used to define a single fluid with variable density and viscosity.

The node-centered control volumes are built from a median dual surrounding each vertex of the mesh. The inviscid fluxes are evaluated using a Roe-averaged flux difference splitting approach, while the gradients required in the viscous terms are evaluated using a local directional derivative technique. Higher order accuracy is achieved via the use of variable extrapolation using gradients computed from a least squares formulation at nodal points. Time stepping is accomplished via a fully implicit second-order accurate backwards Euler approximation, where the resulting linear system is solved by an LU/SGS iterative process. The turbulence models available in the flow solver include the one equation Spalart-Allmaras model, the one equation Menter SAS model, the two-equation q-omega model and the two-equation k-omega/k-epsilon hybrid model (baseline and SST variants) and the Wilcox Stress-omega model. Turbulence equations are decoupled from the solution of the continuity, momentum, and volume fraction equations, i.e., they are loosely coupled with the mean flow. The unstructured solver is parallelized using coarse-grain parallelization with the MPI message-passing library used for the required inter-subdomain communication. Fine grain parallelization is accomplished using loop splitting constructs. A block-Jacobi type updating of the subdomain interfaces ensures efficient parallelization with a small incremental cost incurred in terms of linear sub-iterations required to recover the convergence rate of the sequential algorithm.

The 6DOF response of a ship to waves is predicted in the Tenasi code by integrating elemental shear, pressure, and buoyancy forces over no-slip surfaces at each time step, which together with ship weight gives the resultant force and moment vector. A four-variable quaternion approach is used as described in Pankajakshan et al. (2002). A body-fitted non-inertial reference frame and a fixed inertial coordinate system are used for the angular and translational components of the computation, respectively. In the body-fitted reference frame, the moments of inertia of the model are constants and this greatly simplifies the solution process. The translational velocities and displacements are obtained by directly integrating the accelerations. The quaternion rate equation is solved using a four-stage Runge-Kutta integration scheme. The linear displacements and the attitude quaternion computed at each time step are used to perform a translation and solid-body rotation of the grid for the next time step.

The Tenasi free surface capturing approach has been validated for viscous ship flows at moderate and higher Froude numbers with steep and breaking waves for the R/V Athena, double wedge model, and Wigley hull with incident waves (Wilson et al., 2006c), as well as for simulations with dynamic planar motion mechanism maneuvers for a surface combatant (Wilson et al., 2007b) with results given in Figure 19. Hajjawi et al. (2008) presented RANS calculations using Reynolds stress turbulence models, while Pankajakshan et al. (2007) presented DES calculations of full scale tractor-trailer trucks. Kapadia et al. (2007) performed adjoint-based sensitivity analysis for solid oxide fuel cells.

In Karman and Wilson (2008), a Cartesian-based mesh approach is developed within Tenasi to take advantage of Cartesian meshing away from the hull for automation and adaptation and to provide adequate near-wall viscous spacing at the no-slip surface with reasonably sized grids. The mesh generation approach uses hierarchical Cartesian meshes with general cutting to discretize three-dimensional domains and produce a valid inviscid mesh. Viscous prism layers are subsequently inserted to achieve near-wall turbulence spacing requirements (Karman, 2007). Results for 3D free surface simulations around practical ship geometries are presented with local grid adaption to the free surface and sonar dome vortices in Karman and Wilson (2008). The adapted Cartesian-based mesh is shown in Figure 20, while the predicted wave contours for the

initial and adapted grids are compared with experiment in Figure 21. The Tenasi code is used to study the ship hydroelastic problem in Wilson et al. (2008), where prediction of large amplitude ship motions, water-on-deck and slamming was reported for the ITTC S175 container ship in incident waves as shown in Figure 22. The time-dependent hull forces and moments from the RANS solution were then transferred to the University of Michigan structural analysis group, which predicted the dynamic structural response of the hull to the incident waves (Lee et al., 2008) as shown in Figure 23 and Figure 24. Figure 25 shows a free surface prediction for the Mastercraft CSX-220 planning hull at 23 mph (Fr = 1.0) and at full-scale (Re = 47M). The calculation shows the capability of the Tenasi solver for high speed flow which produces a thin bow sheet and overturning waves. The objectives of the calculation are to predict the free surface wake shape up to two boat lengths behind the stern and to optimize the hull to provide a favorable wake shape for wakeboarding and waterskiing.

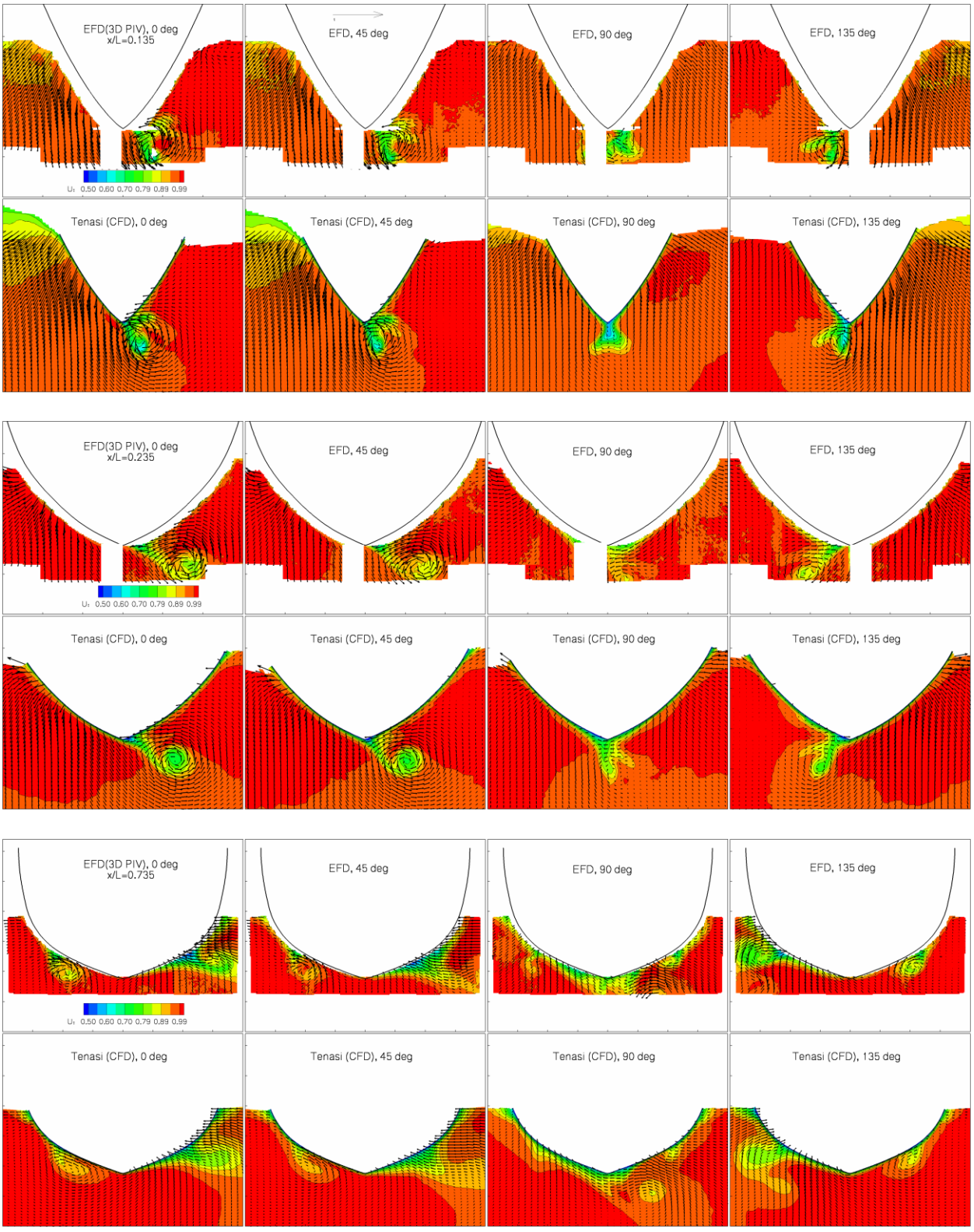

Figure 19 Comparison of *U* contours and *V*-*W* vectors with PIV data for 5512 sway maneuver: *x/L*=0.135 (top), 0.235 (middle), and 0.735 (bottom) from Wilson et al. (2007b)**.**

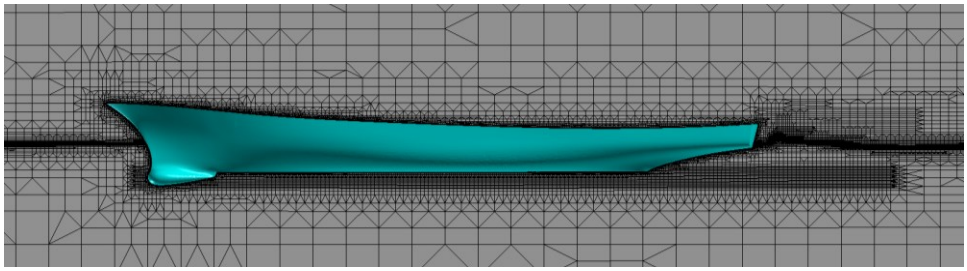

Figure 20 Symmetry plane of free surface adapted mesh from Karman and Wilson (2008).

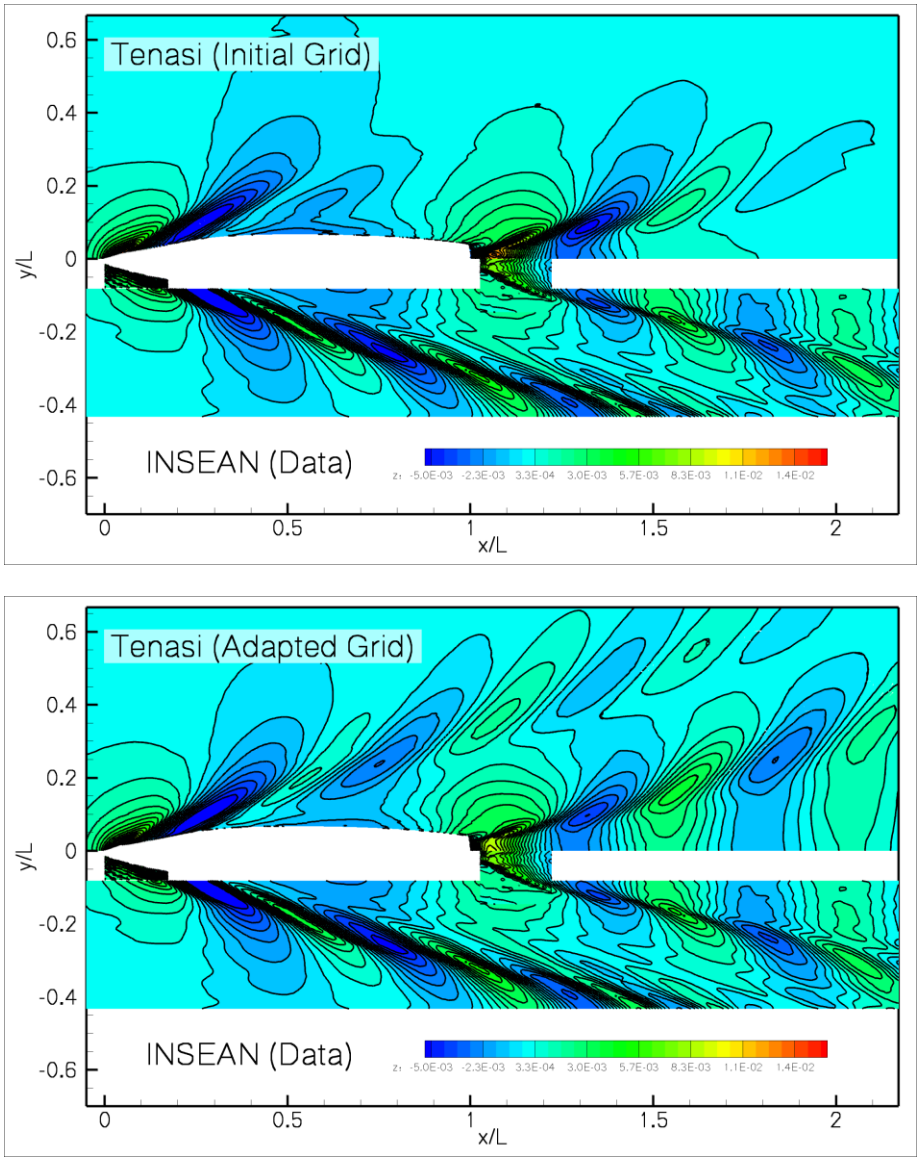

Figure 21 Wave elevation contours for initial (top) and adapted (bottom) Cartesian-based grids compared with data from Karman and Wilson (2008).

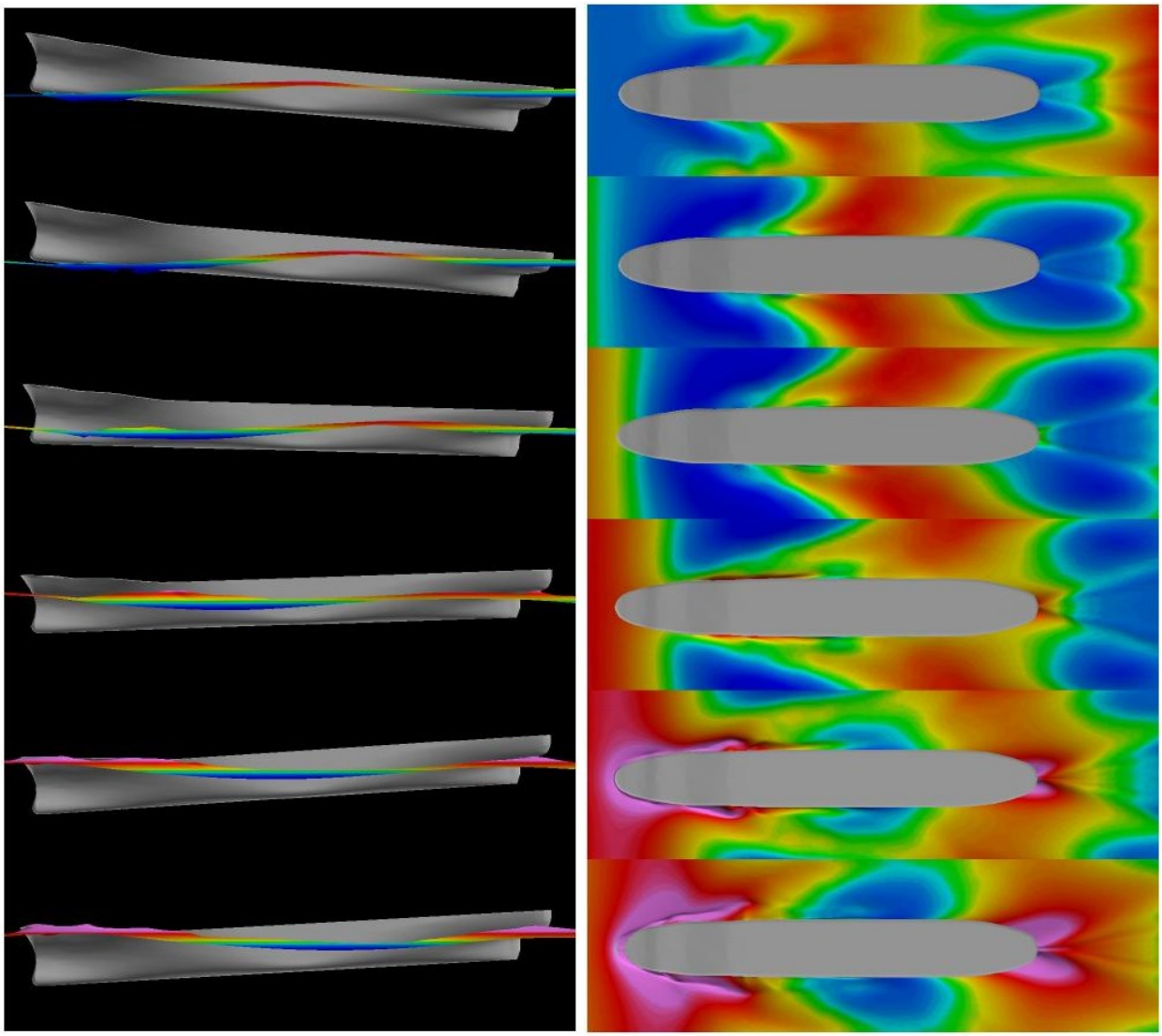

Figure 22 Time sequence of ship slamming: motions and wave contours from maximum pitch up (top most) to maximum pitch down (bottom most).
S175 container ship advancing to the left

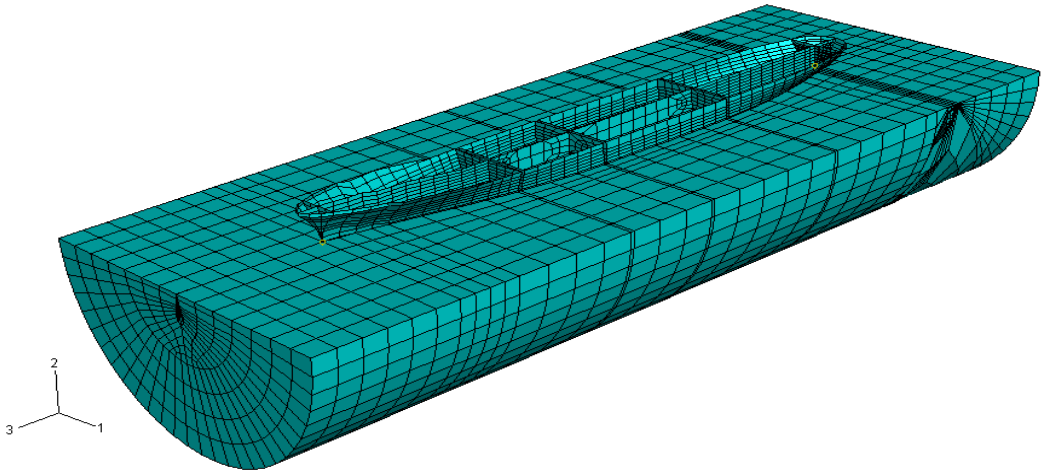

Figure 23 Finite element model for fluid-structure analysis of the S175 container ship.

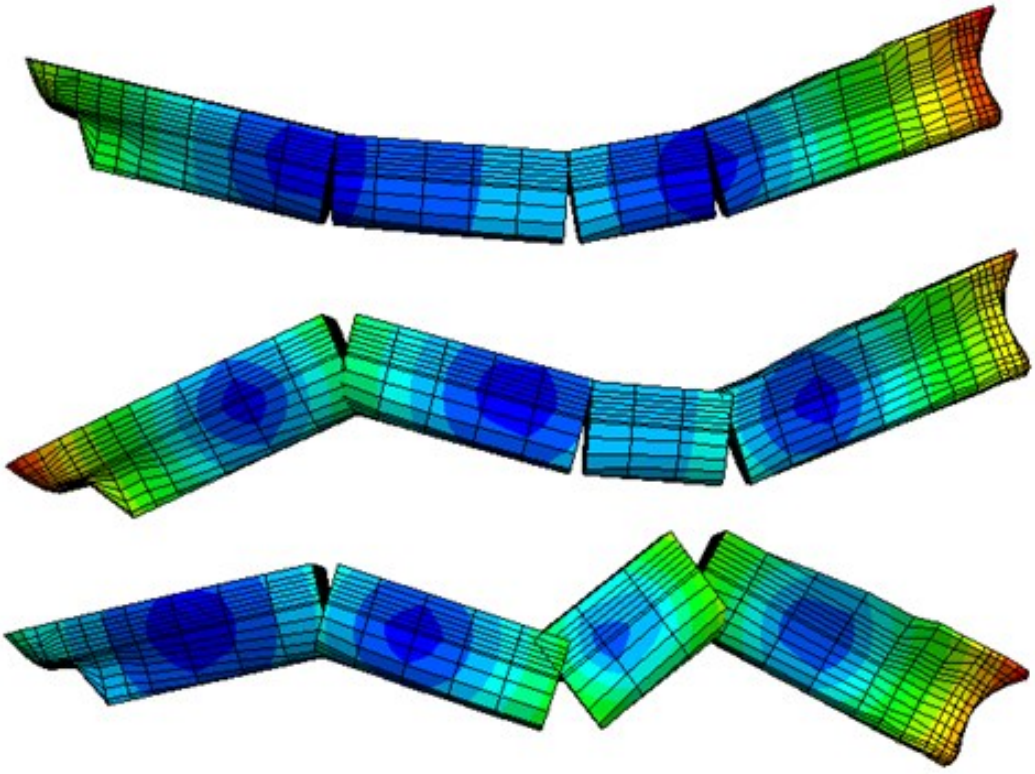

Figure 24 First three flexure modes from the structural analysis of the S175 ship.

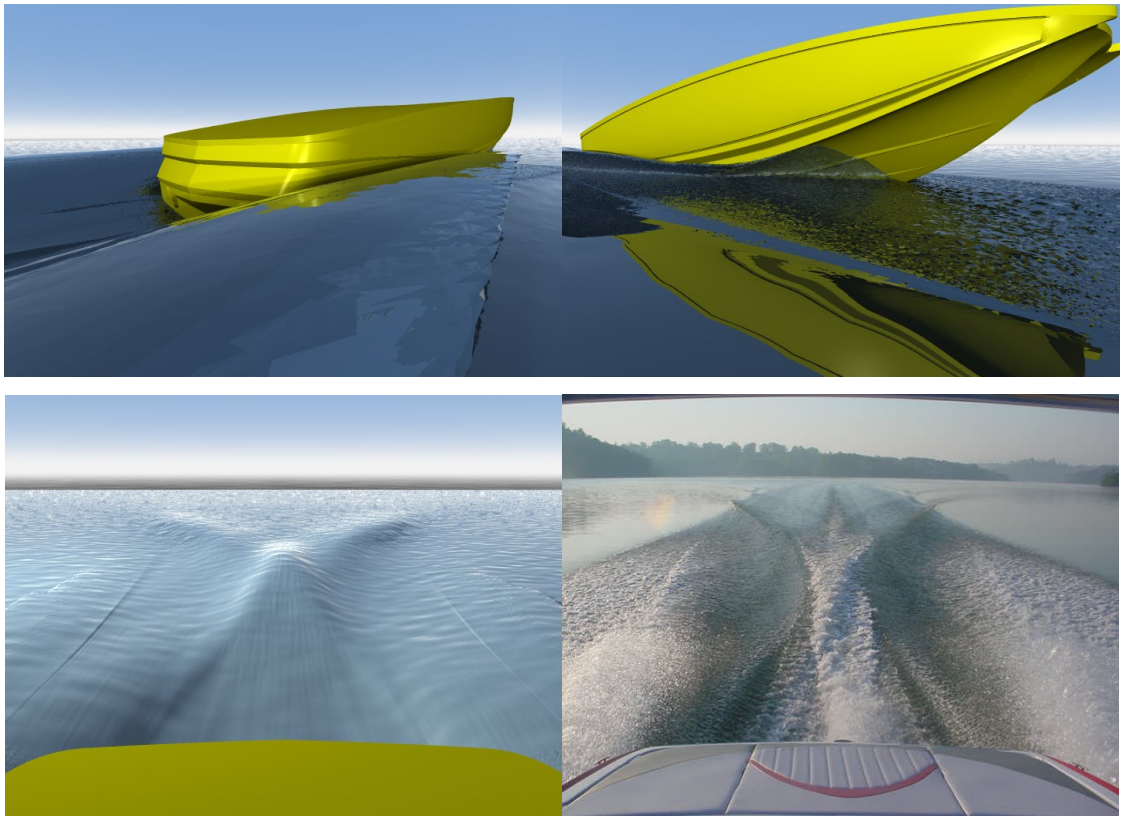

Figure 25 Free surface prediction for the Mastercraft CSX-220 at Fr = 1.0: rear and side perspectives (top) and wake comparison with photo (bottom).

3 CFD Requirements for High Speed Boats

It is often not practical and prohibitively expensive to conduct experimental measurements of full scale ships. A more useful alternative is to carry out experiments using ship models in towing tanks at laboratory scale where conditions can be more easily controlled and repeated. CSH simulations of conventional military ships ($L \sim$ 0 meters) are also typically performed at model scale ($L \sim$ meters) and with medium Froude number ($Fr \sim$), so that predictions can be directly validated using towing tank measurements. For the design of full scale ships, a procedure exists to set model scale experimental conditions based on the full scale design operating condition (Lloyd, 1989). To achieve similarity of gravitational and inertial forces, we require model and full scale Froude numbers to be equal, which leads to the model speed U_{MS} being reduced as

$$U_{MS} = \frac{U_{FS}}{\sqrt{R}} \tag{1}$$

where *MS* and *FS* are used to denote model and full scales, respectively and $R = L_{FS} / L_{MS}$. However, for similarity of viscous forces, the Reynolds number must also be equal at both scales. This requires the model speed to be *increased* as

$$U_{MS} = U_{FS} R \tag{2}$$

Therefore, is impossible to choose a model speed such that inertial, gravitational and frictional forces are dimensionally similar at both scales. In practice, gravitational similarity is more important and practical, so that simulations are performed with Froude number equivalence at model and full scale and with the model scale Reynolds number reduced by the factor $R^{3/2}$

$$\begin{aligned} Fr_{MS} &= Fr_{FS} \\ Re_{MS} &= \frac{Re_{FS}}{R^{3/2}} \end{aligned} \tag{3}$$

The US Navy has shown a recent interest in the development of single and multihull, small, fast, and lightweight boats, i.e., with ship length up to 60 meters and operating speed up to 50 knots. Since novel hull design concepts are being considered, the vast wealth of experimental data and knowledge obtained in the past 30 years for traditional larger ships may not be transferrable, and it is anticipated that CFD will play an increased role in the design of such concepts. Table 2 gives a summary of the *Fr* and *Re* for CFD simulation of conventional ships and fast boats at both model and full scales. Also included are the near-wall spacing required to resolve the turbulent boundary layer down to the no-slip surface and the number of points in the near-wall direction. The estimates are based on typical model scale, fast boat, and conventional ship lengths of 6*m*, 60*m*, and 150*m* and on typical non-dimensional design speeds of *Fr* = 0.3 and 1.1 for the conventional ship and fast boat, respectively. The near-wall spacing $\Delta y / L$ is based on typical isotropic turbulence model requirements of $y^+ = 1$ for the first node off the no-slip surface and the number of points is estimated assuming a constant geometric cell size expansion $E = \Delta y_i / \Delta y_{i-1} = 1.1$ from the no-slip surface (*y/L*=0) to the far-field boundary (*y/L* =1).

Table 2 Physical parameters for conventional ships and fast boats.

	Scale	Length (m)	Speed (m/s)	*Fr*	*Re*	Near-wall spacing, $\Delta y / L$	Required number points
Conventional Ship	Model	6	2.3	0.3	1.45×10^{7}	1.8×10^{-6}	115
	Full	150	12	0.3	1.8×10^{9}	2.3×10^{-8}	161
Fast boat	Model	6	8.4	1.1	5.3×10^{7}	5.4×10^{-7}	128
	Full	60	27	1.1	1.7×10^{9}	2.4×10^{-8}	160

The estimates show that CFD simulations for conventional and fast ships require roughly the same number of grid points to resolve the turbulent boundary layer at full scale. At model scale, the fast boat requires roughly 10% more grid points in the wall normal direction. Because the cell size can be expanded from the no-slip to the far-field boundary, the full scale calculations require only 25% and 40% more grid points for the fast boat and conventional ship, even though the cell size is reduced one and two orders of magnitude, respectively. These estimates of grid counts based on turbulent near-wall spacing requirements for both model and full scales are very reasonable and workable with the current generation of CFD codes and computers. However, at full scale the system of equations may become numerically stiff due to reduced cell size and larger aspect ratio, requiring robust, fully implicit solvers with grid-independent convergence rates (i.e., multigrid, Krylov methods).

Experiments have shown that surface ships operating in calm water and at a low to moderate Froude number ($Fr \le 0.3$) display smooth Kelvin wave patterns with little to no wave breaking. However, wave breaking can occur for $Fr \le 0.3$ with operation in high sea states or with larger amplitude ship maneuvers. Smooth free surfaces can be fully resolved with a reasonable amount of computational resources. An estimate of the axial and transverse cell sizes required to adequately resolve one wavelength of the Kelvin pattern is given by $\Delta x / L \sim$ ~)0. As *Fr* increases, the Kelvin wavelength also increases and fewer points are required to resolve the pattern. Using this

estimate, the conventional ship would require a cell size of roughly $\Delta x / L \sim$ ~ to resolve the smooth Kelvin pattern at Fr = 0.3.

Bow, shoulder, and stern wave breaking will occur at higher Froude number ($Fr \geq 0.4$) to some degree, depending on the shape and slenderness of the geometry. Simulation of breaking waves, which may be required for prediction of spray, under and above water signatures, air entrainment, and bubble formation, requires a free surface capturing approach and an increased amount of computational resources to resolve the complex interfacial topologies that occur. Wilson et al. (2006a) used overlapping grids for the R/V Athena patrol boat in calm water at Fr = 0.43 and determined that a cell size on the order of $\Delta y / L \sim$ ~ was required in the cross plane to resolve the breaking bow and stern waves yielding a total grid count of roughly 7M points. Depending of the purpose of the simulation, the details of the breaking waves may not be important and it may be possible to get a relatively accurate prediction of total resistance within 10-20% using a coarser grid with an order of magnitude less total grid points. Based on the preceding estimates of grid cell sizes, a high-fidelity RANS solution of fast boats at high Fr will require at least an order of magnitude increase in the total grid count compared to that for conventional ships at moderate speed. CFD codes with a local grid refinement capability will allow efficient use of resources by increasing resolution only in the region of the breaking waves.

With regard to seakeeping performance, a CFD code with capability for specifying time dependent inflow conditions for free surface waves and a 6DOF solver will be required to predict ship motions. For higher sea states with wave amplitudes $A > 0.01L$ and wavelength $\lambda \sim$, water on deck and ship slamming are very likely, leading to complex free surface topologies and large ship accelerations. Simulation of such conditions will require a free surface capturing solver with increased levels of robustness, which is often difficult to quantify.

SYMBOLS

λ	Wavelength
A:	Wave amplitude
Fr:	Froude number, $Fr = U / \sqrt{gL}$
g:	Gravitational constant
L:	Ship length
Re:	Reynolds number, $Re = \rho UL / \upsilon$
U:	Ship speed

ABBREVIATIONS

6DOF:	Six-degree-of-freedom
CFD:	computational fluid dynamics
CFDWS05:	CFD Workshop Tokyo 2005
CSH:	computational ship hydrodynamics
CTH:	Division of Hydromechanics at Chalmers University of Technology
DARPA:	Defense Advanced Research Projects Agency
DES:	Detached Eddy Simulation
DTMB 5415:	David Taylor Model Basin surface combatant
G2K:	Gothenburg 2000: A Workshop on Numerical Ship Hydrodynamics
ITTC:	International towing tank conference
KCS:	KRISO container Ship
KRISO:	Korea Research Institute for Ships and Ocean Engineering
KVLCC2:	KRISO container ship
LES:	Large Eddy Simulation
LU/SGS:	Lower-upper/Symmetric Gauss Seidel
MPI:	Message passing interface
NSF ERC:	National Science Foundation, Engineering Research Center
ONR:	Office of Naval Research
PETs:	Portable Extensible Toolkit for Scientific Computation

RANS: Reynolds averaged Navier-Stokes

RS: Reynolds stress turbulence model

REFERENCES

Anderson, W. K., 1992, "Grid Generation and Flow Solution Method for the Euler Equations on Unstructured Grids," Technical Report L-16986, NASA Langley Research Center, Hampton, VA, April 1992.

Anderson, W. K. and Bonhaus, D. L., 1994, "An Implicit Upwind Algorithm for Computing Turbulent Flows on Unstructured Grids," Computers and Fluids, Vol. 23(1), pp. 1-21.

Anderson, W. K., Rausch, R. D., and Bonhaus, D. L., 1995, "Implicit/Multigrid Algorithms for Incompressible Turbulent Flows on Unstructured Grids," AIAA Paper 95-1740.

Balay S., Buschelman K., Gropp W., Kaushik D., Knepley M., Curfman L., Smith B. and Zhang H., 2002, PETSc User Manual, ANL-95/11-Revision 2.1.5, Argonne National Laboratory.

Bensow, R., Fureby, C., Liefvendahl, M., and Persson, T., 2006, "A Comparative Study of RANS, DES and LES," Proc. 26th ONR Symposium on Naval Hydrodynamics, Rome, Italy, 2006.

Briley, W. R., Taylor, L. K., and D. L. Whitfield, 2003, "High-Resolution Viscous Flow Simulations at Arbitrary Mach Number," *J. Comp. Phys*., Vol. 184(1), pp. 79-105.

Carrica, P. Wilson, R., Noack, R., Xing, T., Kandasamy, M., Shao, J., Sakamoto, N., Stern, F., 2006, "A Dynamic Overset, Single-Phase Level Set Approach for Viscous Ship Flows and Large Amplitude Motions and Maneuvering," Proc. 26th ONR Symposium on Naval Hydrodynamics, Rome, Italy, 2006.

Carrica, P., Wilson R., and Stern F., 2007a, "An Unsteady Single-Phase Level Set Method for Viscous Free Surface Flows," Vol. 53, No. 2, *Int. J. Num. Methods Fluids*, Jan. 2007, pp. 229-256.

Carrica, P., Wilson R., Noack, R., and Stern F., 2007b, "Ship Motions using Single-Phase Level Set with Dynamic Overset Grids," Vol. 36, No. 9, *Computers and Fluids*, Jan. 2007, pp-1415-1433.

Cura Hochbaum A, Vogt M., 2002, "Towards the Simulation of Seakeeping and Maneuvering based on the Computation of the Free Surface Viscous Flow," 24th ONR Symp on Naval Hydrodynamics, Fukuoka, Japan, 2002.

Di Mascio, A., Broglia, R., Muscari, R., and Dattola, R., 2004, "Unsteady RANS Simulation of a Manoeuvring Ship Hull," Proc. 25th Symposium on Naval Hydrodynamics, St. John's, Newfoundland and Labrador, Canada, 2004.

Di Mascio, A., Broglia, R., and Muscari, R., 2007, "On the Application of the One–Phase Level Set Method for Naval Hydrodynamic Flows", *Computer and Fluids*, 36(5):868–886.

Dommermuth, D., O'Shea, T., Wyatt, D., Ratcliffe, T., Weymouth, G., Hendrikson, K., Yue, D., Sussman, M., Adams, P., and Valenciano, M., 2007, "An Application of

Cartesian-Grid and Volume of Fluid Methods to Numerical Ship Hydrodynamics," 9th International Conference on Numerical Ship Hydrodynamics, Ann Arbor, Michigan, August 5-8, 2007.

Hajjawi, M., Taylor, L., and Nichols, D., 2008, "Assessment and Modification for Reynolds Stress Transport Turbulence Model Flow Prediction", AIAA-2008-0568, 46th AIAA Aerospace Sciences Meeting and Exhibit, January 2008.

Hay, P. and Visonneau, M., 1995, "Computation of Free-Surface Flows with Local Mesh Adaptation," *Int. J. Num. Methods. Fluids*, 1995 (49), 785-816.

Hino, T. (Editor) 2005, CFD Workshop Tokyo 2005, National Maritime Research Institute, Tokyo, Japan.

Hino, T., Kobayashi, H., and Takeshi, H., 2007, "CFD-Based Design of Ship Hull Forms with Azimuth Propulsion System," 9th International Conference on Numerical Ship Hydrodynamics, Ann Arbor, Michigan, August 5-8, 2007.

Hyams, D., 2000, "An Investigation of Parallel Implicit Solution Algorithms for Incompressible Flows On Unstructured Topologies," Ph.D. Dissertation, Mississippi State University, May 2000.

Hyams, D.G., Sreenivas, K., Sheng, C., Nichols, S., Taylor, L.K., Briley, W.R., and Whitfield, D.L., 2000, "An Unstructured Multielement Solution Algorithm for Complex Geometry Hydrodynamic Simulations," 23rd Symposium on Naval Hydrodynamics, Val de Reuil, France, Sept. 2000.

Kapadia, S, W. K. Anderson and L. Elliott, 2007, "Design and Sensitivity Analysis of Solid Oxide Fuel Cells Using Discrete Adjoint Method", 5th International Energy Conversion Engineering Conference and Exhibit (IECEC), 25 - 27 June 2007, St. Louis, Missouri, AIAA 2007-4832.

Karman, S. L. Jr., 2007, "Unstructured Viscous Layer Insertion Using Linear-Elastic Smoothing," *AIAA Journal*, Vol. 45, No. 1, January 2007, pp. 168-180.

Karman, S. L. Jr. and Wilson, R., 2008, "Hierarchical Unstructured Mesh Generation with General Cutting for Free Surface Simulations," Proceedings of the 27th ONR Symposium on Naval Hydrodynamics, Seoul, Korea, 5-10 Oct. 2008.

Kim, S.-E and Cokljat, D., 2007, "Evaluation of a URANS-LES Hybrid Approach for Turbulent Free-Surface Flows Around Surface-Piercing Bodies," (2007) 9th International Conference on Numerical Ship Hydrodynamics, Ann Arbor, Michigan, August 5-8, 2007.

Larsson, L., Stern, F., and Bertram, V., (Editors) 2002, Gothenburg 2000: A Workshop on Numerical Hydrodynamics, Department of Naval Architecture and Ocean Engineering, Chalmers University of Technology, Gothenburg, Sweden.

Larsson, L., Stern, F., and Bertram, V., 2003, "Benchmarking of Computational Fluid Dynamics for Ship Flows: The Gothenburg 2000 Workshop," *Journal Ship Research*, Vol. 47, No. 1, March 2003, pp. 63-81.

Lee, D., Maki, K., Wilson, R., Troesch, A., and Vlahopoulos, N., 2008, "Dynamic Response of a Marine Vessel Due to Wave-Induced Slamming," Int. Sym. On Vibro-

Impact Dynamics of Ocean Systems and Related Problems, Troy, Michigan, 2-3 Oct. 2008.

Lloyd, A., 1989, Seakeeping: Ship Behaviour in Rough Weather, Ellis Horwood Series in Marine Technology, Ellis Horwood Ltd.

Maki, K., Doctors, L, Rhee, S., Wislon, W., Beck, R., and Troesch, A., 2007, "Resistance Prediction for a High-Speed Sealift Trimaran," 9th International Conference on Numerical Ship Hydrodynamics, Ann Arbor, Michigan, August 5-8, 2007.

Nichols, D., 2002, "Development of a Free Surface Method Utilizing an Incompressible Multi-Phase Algorithm to Study the Flow About Surface Ships and Underwater Vehicles," PhD Dissertation, Mississippi State University, August 2002.

Noack R., 2005, "SUGGAR: a General Capability for Moving Body Overset Grid Assembly," AIAA paper 2005-5117, 17th AIAA Computational Fluid Dynamics Conf., Toronto, Ontario, Canada.

Noack, R., 2007, "Enabling Large Amplitude and Relative Motions Through Overlapping Grids," 9th International Conference on Numerical Ship Hydrodynamics, Ann Arbor, Michigan, August 5-8, 2007.

Orihara H and Miyata H., 2003, "Evaluation of Added Resistance in Regular Incident Waves by Computations Fluid Dynamics Motion Simulation Using Overlapping Grid System," *J. Marine Science and Technology* 2003; 8:47-60.

Paik, K-J., Maki, K., Choi, H., Vlahopoulos, N., Carrica, P., and Troesch, A, 2008, "CFD-Based Method for Structural Loads on Surface Ships," Proceedings of the 27th ONR Symposium on Naval Hydrodynamics, Seoul, Korea, 5-10 Oct. 2008.

Pankajakshan, R. and Briley, W. R., 1995, Parallel Solution of Viscous Incompressible Flow on Multi-Block Structured Grids Using MPI. Parallel Computational Fluid Dynamics: Implementations And Results Using Parallel Computers, pages 601-608.

Pankajakshan, R., Remotigue, M. G., Taylor, L. K., Jiang, M., Briley, W. R., and D. L. Whitfield, 2002, "Validation of Control-Surface Induced Submarine Maneuvering Simulations Using UNCLE," 24th Symposium on Naval Hydrodynamics, Fukuoka, Japan, July 8-13, 2002.

Pankajakshan, R. Kidambi Sreenivas, Brent Mitchell, and David L. Whitfield, 2007, "CFD Simulations of Class 8 Trucks," 2007-01-4293, SAE 2007 Commercial Vehicle Engineering Congress & Exhibition, October 2007.

Tahara, Y., Campana, E., Peri, D., Pinto, A., Kandasamy, M., and Stern, F., 2007, "Global Optimization and Variable Fidelity Strategies in the Single and Multiobjective Optimal Design of Fast Multihull Ships," 9th International Conference on Numerical Ship Hydrodynamics, Ann Arbor, Michigan, August 5-8, 2007.

Visonneau, M., Deng, G., Quentey, P., 2006, "Computation of Model and Full Scale Flows Around Fully-Appended Ships with an Unstructured RANSE Solver," Proc. 26th ONR Symposium on Naval Hydrodynamics, Rome, Italy, 2006.

Wilson R., Carrica, P., and Stern F., 2006a, "URANS Simulation for a High-Speed Transom Stern Ship with Breaking Waves," Vol. 20, No. 2, *Int. J. of CFD*, 2006, pp. 105-125.

Wilson R., Carrica, P., and Stern F., 2006b, "Unsteady RANS Method for Ship Motions with Application to Roll for a Surface Combatant," *Computers and Fluids*, 2006, Vol. 35, pp.501-524.

Wilson, R., Nichols, D.S., Mitchell, B., Karman, S.L., Hyams, D.G., Sreenivas, K., Taylor, L.K., Briley, W.R., and Whitfield, D.L., 2006c, "Application of an Unstructured Free Surface Flow Solver for High Speed Transom Stern Ships," 26th Symposium on Naval Hydrodynamics, Rome Italy, September. 17-22, 2006.

Wilson, W., Fu., T., Fullerton, A., and Gorski, J., 2006d, "The Measured and Predicted Wave Field of Model 5365: An Evaluation of Current CFD Capability," Proc. 26th ONR Symposium on Naval Hydrodynamics, Rome, Italy, 2006.

Wilson R., Carrica, P., and Stern F., 2007a, "Simulation of Ship Breaking Bow Waves and Induced Vortices and Scars," Vol. 54, No. 4, *Int. J. Num. Methods Fluids*, June 2007, pp. 419-451.

Wilson, R., Nichols, S., Mitchell, B., Karman, S., Betro, V., Hyams, D., Sreenivas, K., Taylor, L., Briley, R., and Whitfield D., 2007b, "Simulation of a Surface Combatant with Dynamic Ship Maneuvers," 9th Int. Conf. in Num. Ship Hydro., University of Michigan, 5-8 Aug. 2007.

Wilson, R., Lei, J., Karman, Jr., S., Hyams, D., Sreenivas, K., Taylor, L., and Whitfield D., 2008, "Simulation of Large Amplitude Ship Motions for Prediction of Fluid-Structure Interaction," Proceedings of the 27th ONR Symposium on Naval Hydrodynamics, Seoul, Korea, 5-10 Oct. 2008.

Xing, T., Shao, J., and Stern, F., 2007, "BKW-RS-DES of Unsteady Vortical Flow for KVLCC2 at Large Drift Angles," 9th International Conference on Numerical Ship Hydrodynamics, Ann Arbor, Michigan, August 5-8, 2007.

Yang, C., Lu, H., Lohner, R., Liang, X., and Yang, J., 2007, "An Unstructured Grid Based VOF Method for Ship Motions Induced by Extreme Waves," 9th International Conference on Numerical Ship Hydrodynamics, Ann Arbor, Michigan, August 5-8, 2007.

Yang, J., Sakamoto, N., Wang, Z., Carrica, P., and Stern, F., 2007, "Two-Phase Level-Set/Immersed-Boundary Cartesian Grid Method for Ship Hydrodynamics," 9th International Conference on Numerical Ship Hydrodynamics, Ann Arbor, Michigan, August 5-8, 2007.